2741-19 in combination with piperaquine as next generation therapy against *P. falciparum*

By
Brooke Skinner
Computational Biology, ScB, Brown University, 2023

Thesis
Submitted in partial fulfillment of the requirements for the Degree of Master of Science
in the Graduate Program of Biotechnology at Brown University

PROVIDENCE, RHODE ISLAND
May 2026

This thesis by Brooke Skinner is accepted in its present form by the Graduate Program in Biotechnology as satisfying the thesis requirements for the degree of Master of Science

Date Apr 30, 2026 Signature: Jonathan Kurtis, MD, PhD (Apr 30, 2026 14:01:28 EDT)

Dr. Jonathan Kurtis, Advisor

Date Apr 30, 2026 Signature: Tanbir Najrana (Apr 30, 2026 13:57:59 EDT)

Dr. Tanbir Najrana, Reader

Date Apr 30, 2026 Signature: HANNAH WEI WU (Apr 30, 2026 13:58:56 EDT)

Dr. Hannah Wu, Reader

Approved by the Graduate Council

Date _____ Signature: _____

Dr. David Lindstrom, Dean of the Graduate School

Acknowledgments

I want to first thank my advisor, Dr. Jonathan Kurtis. Dr. Kurtis gave me the opportunity to fall in love with wet lab and translational global health research nine months ago. I now cannot imagine doing anything else. Dr. Kurtis has exceeded all expectations of mentorship, providing endless opportunities for me to develop as a scientist, including supporting my research ideas for this master's thesis. His leadership and guidance came at a critical time in my early career development and have changed the trajectory and success of my career immeasurably. I would also like to thank my thesis readers, Dr. Tanbir Najrana and Dr. Hannah Wu for their scientific guidance and support. Along with Dr. Brajesh Singh, they provided significant help in my execution of this project from experimental design to data analysis and interpretation. I would like to deeply thank each member of the Kurtis Lab. Specifically, I want to extend the utmost gratitude to the members that spent countless hours training and collaborating with me: Alan Ardito, Aidan Biondi, Lillianna Hammons, Kanika Men, and Samantha Maguire. You are all inspiring and impressive scientists and even more impressive friends. I am exceptionally grateful that we have crossed paths in the Kurtis Lab. My decision to embark on this research last spring would not have been possible without the support and encouragement from four special childhood friends that believe in me beyond what I can even imagine for myself. I would also like to thank my sister, parents, and family for instilling the importance of education and work ethic that has driven me from a young age. This thesis would not be possible without each of you.

Table of Contents

Table of Figures

Table of Tables

Abstract of "2741-19 in combination with piperaquine as next generation therapy against P. falciparum," by Brooke Skinner, ScM, Brown University, May 2026.

Introduction: Malaria, caused by the *Plasmodium* parasite, is a leading cause of mortality in sub-Saharan Africa, disproportionately affecting children under the age of 5. The species *Plasmodium falciparum* is responsible for > 95% of these deaths. Recent spread of drug resistance in Africa to the mainstays of malaria treatment, artemisinin combination therapy (ACT), underscores the importance of novel antimalarial compound development. The Kurtis Lab at Brown University previously identified families of antimalarial small-molecule compounds believed to target *P. falciparum* glutamic acid rich protein (PfGARP). 2741-19 is the most effective compound with an IC_{50} around 50 nM. Part II investigates 2741-19 drug binding with *P. falciparum* proteins to support mounting evidence that 2741-19 kills *P. falciparum* via PfGARP binding, an independent mechanism of action from artemisinin derivatives and ACT partner drugs. Part III assesses the potential for *in vitro* synergistic killing of *P. falciparum* between short acting 2741-19 and longer lasting ACT partner drugs widely used in Africa, lumefantrine and piperaquine. **Methods:** Drug binding enzyme-linked immunosorbent assays (ELISA) were performed over 72 hours examining binding between a variety of *Plasmodium* proteins and antimalarial compounds. Growth inhibition assays designed with dose-response matrix dilutions were conducted and four mathematical models (i.e., ZIP, HSA, Loewe Additivity, Bliss Independence) were utilized to assess *in vitro* synergistic killing. **Results:** 2741-19 showed over 4X higher binding to PfGARP via optical density (OD) measurements than other antimalarials and statistical significance compared to controls ($p < 0.0001$). 2741-19 and piperaquine synergistically kill *P. falciparum in vitro* across relevant synergy models, with highest scoring in the Bliss Independence model. **Conclusions:** Differential binding of 2741-19 to PfGARP in ELISAs is consistent with 2741-19 binding to PfGARP in its mechanism of killing

action, unique from current clinically utilized antimalarials. Highest *in vitro* synergy scoring with piperaquine in the Bliss Independence model supports the notion that these compounds operate on unique pathways to inhibit *P. falciparum* growth and proliferation. These findings support further evaluation of 2741-19 and piperaquine as promising candidates for the next generation of antimalarial combination treatments.

Part I: Introduction and Scientific Premise

Chapter 1: Introduction

1.1.1 Plasmodium Parasite Lifecycle

Malaria is a parasitic vector-borne disease transmitted to humans from the bite of a female *Anopheles* mosquito infected with the *Plasmodium* parasite. Of the 200+ described *Plasmodium* species, only five infect humans: *P. falciparum, P. vivax, P. knowlesi, P. malariae,* and *P. ovale.*[1] Regardless of species, *Plasmodium* essentially has the same life cycle across vector and human host. As seen in Figure 1, once an infected mosquito takes a blood meal, she transmits sporozoites into the body that target the liver for the first stage of human infection, the exoerythrocytic stage. Infected hepatocytes can contain up to 40,000 parasites.[2] Within hepatocytes, sporozoites develop into hepatic schizonts, which rupture the hepatic cell after 5 to 25 days[3] and release merozoites that target red blood cells, or erythrocytes.[4] Inside the infected erythrocyte, the parasite's developed morphology resembles a ring before growing a digestive vacuole and becoming a trophozoite. The digestive vacuole enables the parasite to break down hemoglobin. Parasites develop from trophozoites to schizonts, initiating another cycle of cell rupture, merozoite release, and rapid infection of other erythrocytes.[4] This asexual blood stage of *Plasmodium* infection causes the clinical and physical symptoms of malaria. Shown in Figure 1, most antimalarials molecularly target the asexual blood stage to inhibit parasite reproduction and alleviate disease.

From the erythrocytic life cycle, some parasites will selectively develop from trophozoites into intraerythrocytic gametocytes in a process called gametocytogenesis. This initiates the sexual stage of the parasite life cycle approximately 7-14 days following initial infection.[5] The sexual life stage can also be initiated when the parasites are under significant

stress in the host and receive environmental signals including parasite density, anemia, host immune response, or drug treatment.[5] In *P. falciparum* specifically, gametocytes develop over the course of 10 days, which is about 5 times longer than other *Plasmodium* species.[5] Gametocytes hide in the body until another *Anopheles* mosquito takes a blood meal and has the opportunity to infect a new vector, or mosquito. This newly infected mosquito restarts the *Plasmodium* lifecycle.

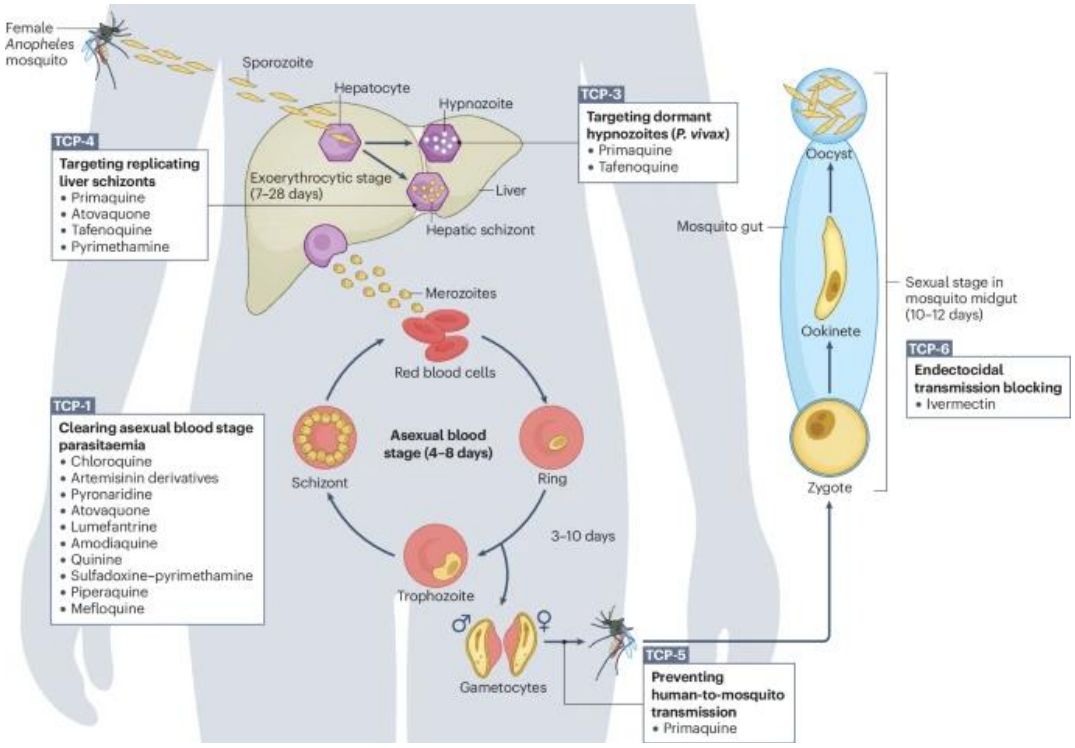

Figure 1 Antimalarial drug targeting during lifecycle of the *Plasmodium* parasite in human hosts. Reproduced from Okombo, et al. (2025).[6] Parasites are deposited into the body from the blood meal of a female *Anopheles* mosquito blood meal and first infect liver cells in the exoerythrocytic stage. Target candidate profile (TCP) 1 highlights the priority of drugs that clear parasites in the asexual blood stage of development. Antimalarials, piperaquine and lumefantrine, target the asexual blood stage of infection and we assessed for synergistic interactions with novel compound 2741-19.[6]

1.1.2 Global Burden of Malaria

Malaria is one of the largest single-agent causes of mortality in low-middle income countries[1], with the WHO reporting 282 million cases in 2024 and over 600,000 deaths across 80 countries.[7] The most prevalent *Plasmodium* species are *P. falciparum* and *P. vivax,* where *P.*

falciparum is the dominant species in sub-Saharan Africa and *P. vivax* is most prevalent outside of sub-Saharan Africa.[1]

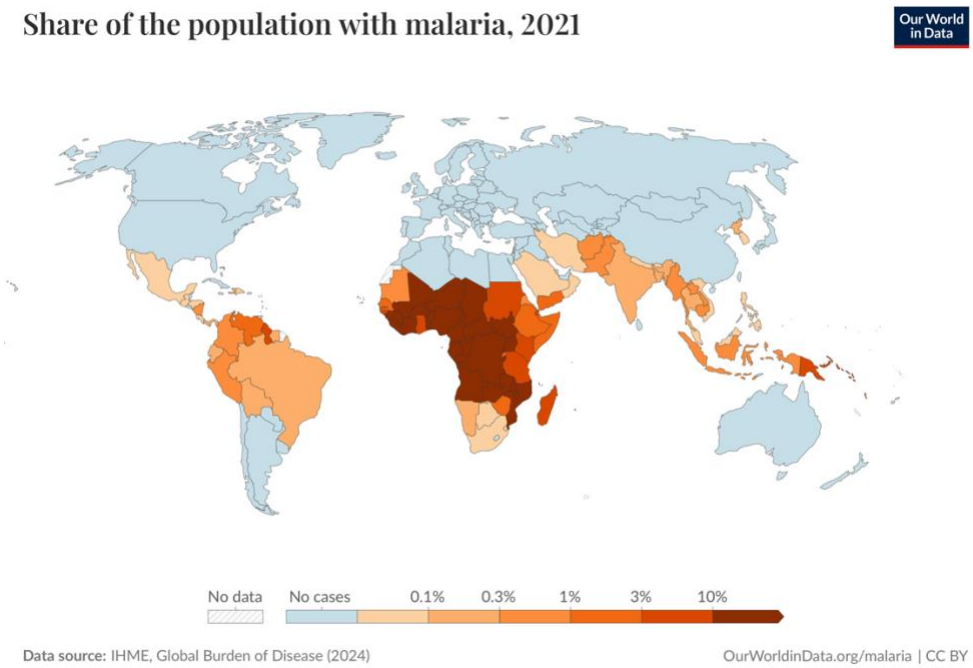

Figure 2 Share of country populations with malaria in 2021 as reported by the Institute for Health Metrics and Evaluation (IHME). [8]

Plasmodium falciparum is responsible for more than 95% of all malaria deaths. Africa bears over 94% of the global malaria disease burden and mortality with the WHO reporting 265 million cases and 579,000 deaths in 2024 (Figure 2).[1] Malaria is diagnosed as either mild/uncomplicated or severe depending on its clinical manifestation and measured parasitemia. Mild malaria cases are categorized by symptoms such as fever, chills, and headaches whereas severe malaria (SM) patients exhibit high parasitemia (> 5%), and clinical symptoms such as seizures, impaired consciousness, and acidosis.[7] While malaria infects people at all ages, children under 5 are disproportionately vulnerable to severe malaria, accounting for 75% of all malaria deaths in Africa.[1] Adults infected with malaria in endemic regions are commonly asymptomatic or mildly infected due to acquired immunity from exposure and repeated infection. This observed acquired immunity to severe malaria *P. falciparum* infections provides a lens into host-

parasite interactions that could be leveraged for severe malaria preventative or therapeutic measures.

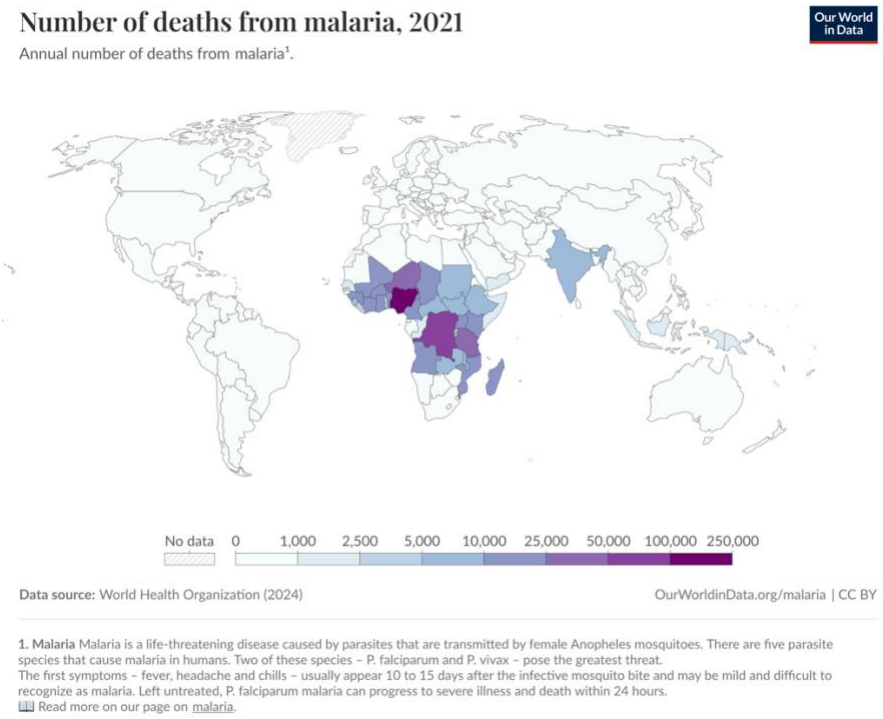

Figure 3 Global prevalence of malaria deaths in 2021 as reported by the IHME. Sub-Saharan Africa is disproportionately burdened with mortality from malaria.[9]

1.1.3 Current Malaria Treatment and Increasing Drug Resistance

From the 17th to mid-20th centuries, quinine was primarily used to treat all malaria infections.[10] Resistance to quinine was first reported in the mid-1900s, catalyzing the development and therapeutic use of chloroquine and other antimalarials globally.[10] Specifically, a Chinese drug discovery program in 1972 identified extracts of sweet wormwood, *Artemisia annua,* had strong antimalarial activity in mice, leading to the discovery of the current backbone of clinical malaria treatment, artemisinin, and its many analogs.[11]

Elimination half-life is defined as the time it takes for a compound's concentration in the blood plasma to decrease by 50%.[12] Artemisinin specifically has an elimination half-life of 2 to 5 hours.[13] Both a strength and weakness of artemisinin therapy is its short elimination half-life in

the body. While this means antimalarial activity is delivered quickly to patients, it provides opportunity for the development of erythrocytic drug resistance. With an elimination half-life ranging from under 1 hour for artesunate and up to 11 hours for artemether, the rapid action and clearance rate of artemisinin and its derivatives can lead to resistance events over the allotted course of treatment.[13]

Partial artemisinin resistance (ART-R) was first seen in the Greater Mekong region of Southeast Asia in 2008.[11] ART-R is caused by mutations in the *P. falciparum* Kelch13 (K13) protein and independent resistance events have since been seen in various African countries.[11] In the WHO's 2025 malaria report, they stress this increasing threat of antimalarial drug resistance, highlighting partial resistance to artemisinin derivatives in 8 African countries and signs of declining ACT partner drug efficacy.[14] Partial resistance to both artemisinin derivatives and partner drugs leads to a significant decline in treatment efficacy, rendering ACT ineffective.[15] Partial resistance to any antimalarials treating *P. falciparum* is especially concerning in Africa, which bears a disproportional burden of *P. falciparum* infections and mortality compared to other regions. Shown in Figure 4, by the start of the 20th century, the prevalence of drug resistance to monotherapies necessitated the development and widespread use of combination antimalarial therapies.

To combat resistance and increase treatment success, artemisinin and other monotherapies are administered alongside longer lasting antimalarial compounds. The most clinically utilized artemisinin-based combination therapies (ACTs) for uncomplicated malaria in Africa are artemether-lumefantrine (AL), artesunate–amodiaquine (AS-AQ), dihydroartemisinin–piperaquine (DHA-PPQ), and pyronaridine–artesunate (PA), with AL and DHA-PPQ as the mainstays of clinical treatment in Kenya, where our research colleagues at the

Kenya Medical Research Institute (KEMRI) are based. Lumefantrine has an elimination half-life of 3 to 6 days depending on the patient's infection status[16] and piperaquine's elimination half-life is reported around 33 days.[17] In this research, we focus on assessing lumefantrine and piperaquine as potential partner drugs to the novel compound 2741-19 based on their widespread clinical usage in Kenya and reported developing drug resistance globally.[18,19]

In the past years, reports of resistance to ACT partner drugs have increased in Africa. Researchers have linked increased copy number of *pfmdr1×N* as a genetic marker of decreased artemether-lumefantrine treatment efficacy, highlighting the increasing *P. falciparum* tolerance to treatment measures.[20] *P. falciparum* parasites with increased copy numbers of plasmepsin-coding genes (*pfpm*) has been linked to piperaquine resistance in clinical practice.[21] To reduce the chance of resistance events, it is imperative that drugs used in combination kill parasites through different mechanisms of action. This ensures that if resistance is developed to one of the drugs, it is unlikely to result in treatment failure and can still effectively clear parasitic infection. Recently, with the mounting threat of ART-R, approaches in treatment have considered therapeutic options outside of the ACT paradigm. Current antimalarial innovation includes non-artemisinin based combination therapy, such as the development of GanLum, a ganaplacide-lumefantrine combination therapy in clinical stage evaluation from Novartis.[22]

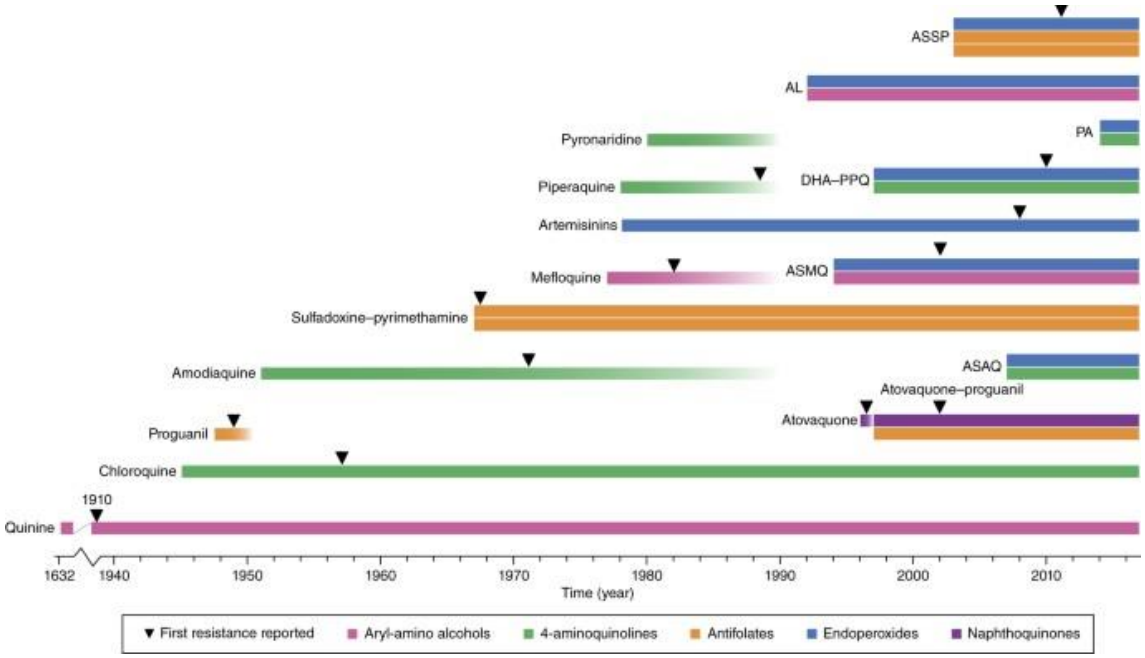

Figure 4 Timeline of antimalarial monotherapy and combination therapy strategies with documented resistance events. Quinine was the first compound used to treat malaria with the first resistance events reported in the early 20th century. By the latter half of the 20th century, clinicians started treating malaria with multiple antimalarials, starting with the sulfadoxine-pyrimethamine combination. The discovery of artemisinin and its derivatives in the late 1970's catalyzed the current mainstay of antimalarial treatment, artemisinin combination therapy (ACT).[10]

1.1.4 Molecular Targets and Mechanisms of ACT Antimalarials

Many antimalarial drugs, including artemisinin and piperaquine, are thought to work by preventing the detoxification of heme (Figure 5). Within the digestive vacuole, parasites reduce hemoglobin into amino acids that can be utilized for parasite protein synthesis and thus growth.[10] As a byproduct of this process, heme containing Fe^{2+} is oxidized to Fe^{3+} protoporphyrin (FPIX), which induces toxic oxidative stress for the parasite.[10] In a healthy parasite, FPIX is detoxified in its incorporation to hemozoin crystals.[10] Drugs that block the detoxification of heme into chemically inert hemozoin crystals or disrupt this process in other ways result in a fatal buildup of toxic heme in the parasite.

Artemisinin exerts its antimalarial activity through a heme-dependent activation process within the malaria parasite. Heme activates artemisinin's antimalarial activity by cleaving its endoperoxide bridge, generating highly reactive intermediates that indiscriminately alkylate

nearby biomolecules, leading to widespread cellular damage and parasite death.[23,24] In contrast, piperaquine, and other 4-aminoquinolines, act primarily within the parasite's digestive vacuole interfering with heme detoxification and preventing the conversion of toxic free heme into inert hemozoin. Thus, although both drug classes are associated with heme biology, their mechanisms of action are fundamentally distinct: artemisinin relies on heme-mediated activation to produce broad cytotoxic damage, whereas 4-aminoquinolines target heme detoxification pathways to disrupt parasite survival within the digestive vacuole (Figure 5).[25]

The mechanisms of action for antimalarials in clinical use are not always fully understood. Lumefantrine, for example, despite being used for decades does not have a clearly defined mechanism of action for parasite killing, but may also work on the heme detoxification pathway.[26] To prevent resistance events, it is crucial that the next generation of antimalarials have unique mechanisms of action.[6]

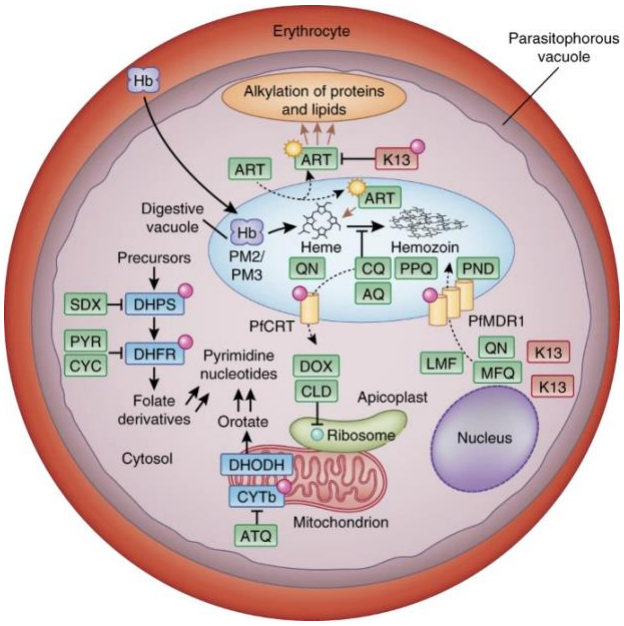

Figure 5 Molecular targets of clinically relevant antimalarial drugs and their mechanisms of resistance.[10] Artemesinin (ART), piperaquine (PPQ), and lumefantrine (LMF) are all pictured to interact in different ways with the heme to hemozoin detoxification pathway.

1.1.5 PfGARP Target Identification

To understand the disproportionate fatality burden of *P. falciparum* infection on children and the observed acquired immunity against severe malaria, researchers in the Kurtis Laboratory at Brown University used a differential screening method to compare antibody responses of children susceptible and resistant to severe malaria from *P. falciparum* parasites. Using plasma from a Tanzania birth cohort, they identified antibodies against *P. falciparum* glutamic acid rich protein (PfGARP) were present in children resistant to severe malaria but absent in plasma samples of children susceptible to severe malaria.[27] Longitudinal cohort studies in Tanzanian children (n = 246) shows those without anti-PfGARP antibodies had a 2.5 times higher risk of having severe malaria.[27]

PfGARP is a parasite antigen present in only *P. falciparum* parasites on the exofacial surface of infected erythrocytes during trophozoite stage. These results were consistent with higher anti-PfGARP antibody density predicting decreased parasitemia in serum samples from Kenyan males aged 12 to 35 years old (n = 135).[27] Furthermore, the Kurtis Laboratory determined anti-PfGARP antibodies inhibit parasite growth in culture and non-human primate vaccination with PfGARP provides some protection against infection.[27]

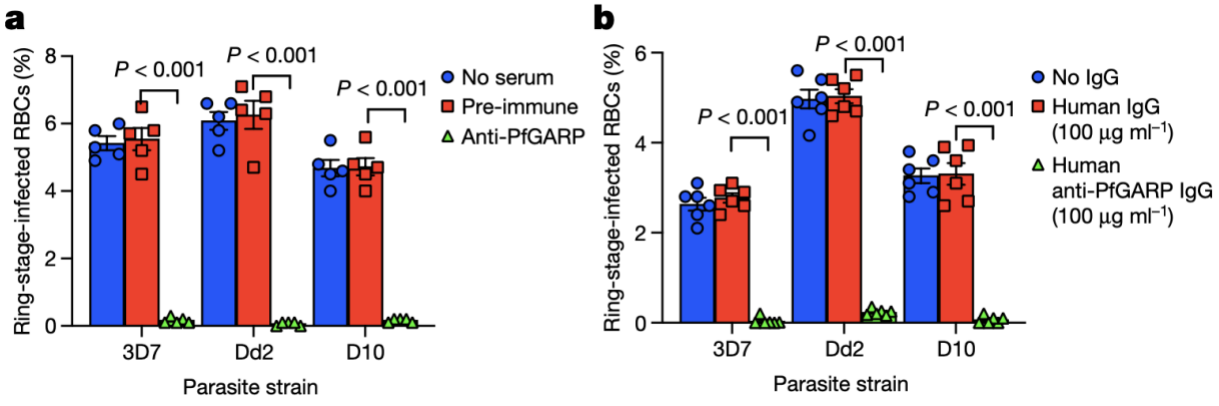

Figure 6 Anti-PfGARP antibodies inhibit *P. falciparum* parasite growth.[27]

The Kurtis Laboratory demonstrated the potential of anti-PfGARP antibodies in mRNA vaccination for malaria.[27] Given the killing ability of anti-PfGARP (Figure 6), PfGARP as a target could have therapeutic and prophylactic value in *P. falciparum* infection management. The complete inhibition of parasite growth in anti-PfGARP red blood cells (RBCs) shown in Figure 7, suggests PfGARP binding is sufficient for parasite killing. The accessible presentation of PfGARP on the surface of infected erythrocytes makes it a prime potential therapeutic target. Additionally, PfGARP has no homology to host proteins, limited sequence variation,[28] and is present during the asexual blood stage of the parasite, satisfying one of the crucial priorities of malaria drug development as described by Blasco, et al.[10] Shown in Figure 7, PfGARP is essential for *in vivo* parasite growth and development. Its exact mechanistic purpose as a specific protein of *P. falciparum,* however, is not well characterized or understood.

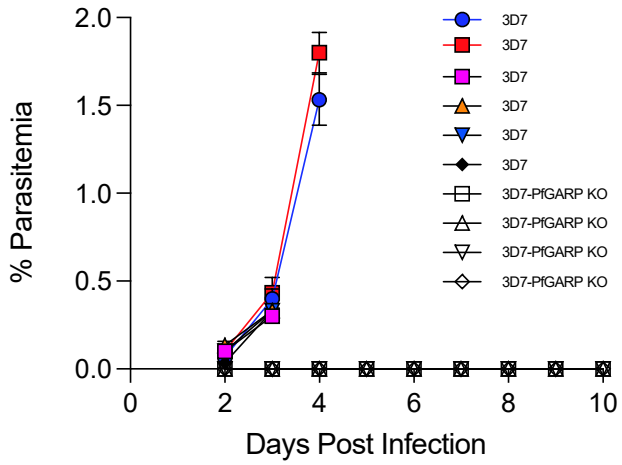

Figure 7 Measured *in vivo* parasitemia of *P. falciparum* 3D7 strain and 3D7-PfGARP knockout strains in infected NSG murine model.

1.1.6 Small-Molecule Drug Development Targeting PfGARP

To assess the therapeutic potential of PfGARP as a druggable target in *P. falciparum* infection, the Kurtis Laboratory conducted a high-throughput bead-based fluorescence screening of 30-million small molecules from the Torrey Pines Combinatorial Library. Low fluorescence

indicated limited ability of anti-PfGARP to bind to PfGARP coated beads, signaling the small-molecule compound successfully binding with PfGARP. Sub-libraries of the lowest fluorescence scaffolds were identified and screened for *P. falciparum* killing activity. Multiple families of effective *P. falciparum* growth inhibiting compounds were identified in this way, including 2741, a family of 36 compounds. 2741-19 was selected for further development as one of the most potent compounds, with an IC_{50} around 50 nM (Figure 8). Pharmacokinetic (PK) evaluation of 2741-19 *in vivo* studies in *Aotus* monkeys showed a half-life of approximately 38 hours. The half-life of 2741-19 is a comparable PK profile to artemisinin and its derivatives than ACT partner drugs.

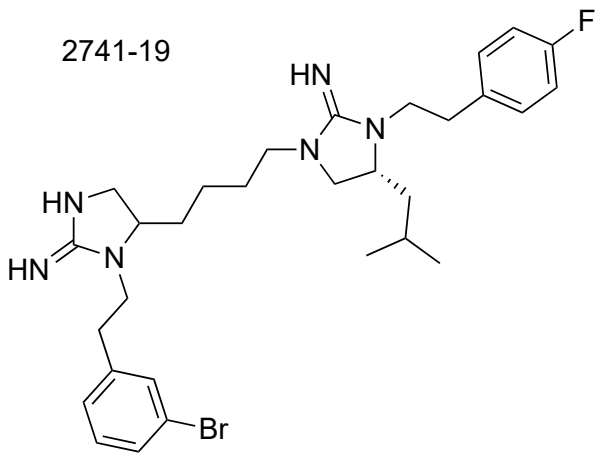

Figure 8 Chemical structure of novel compound 2741-19.

1.1.7 Scientific Premise

Considering the tenants of malaria partner drug therapy, this research assesses whether novel small-molecule compound 2741-19 could be developed as a combination therapy with commonly utilized antimalarial ACT partner drugs. The fast-acting half-life and killing efficacy of 2741-19 suggests it could be used in lieu of or similarly to artemisinin and its derivatives. This

research aims to investigate whether 2741-19 has a unique mechanism of action from the selected partner drugs in assessment (Part II) and if so, whether there are *in vitro* synergistic effects between 2741-19 and selected partner drugs (Part III). *In vitro* synergistic interaction can be used as rationale for choosing one partner drug over another for *in vivo* assessment. Lumefantrine and piperaquine were selected as the primary partner drugs for evaluation with 2741-19 given their predominance in *P. falciparum* ACT therapy in Africa, which disproportionately bears the burden of infections globally.

Part II: 2741-19 differentially binds to PfGARP compared to ACT antimalarial drugs

Abstract

Infections of *P. falciparum* malaria are responsible for > 95% of the ~600,000 deaths attributed to malaria annually, a majority of which are children under the age of 5. Increasing drug resistance necessitates antimalarial treatment of multiple drugs with unique targets, currently known as artemisinin combination therapy (ACT). Previous research in the Kurtis Laboratory shows binding of exofacial *P. falciparum* antigen PfGARP and novel small-molecule antimalarial 2741-19, however, it is unknown whether there is compound specific binding of 2741-19 and PfGARP. This distinction is important because it supports claims that there are separate mechanisms of action for parasite killing between 2741-19 and current antimalarials, a requirement of antimalarial combination therapy. To assess this, we evaluated 2741-19 binding with other compounds (i.e., 2741-19 analog 13, MT 2-20, DHA, lumefantrine, and piperaquine) in enzyme-linked immunosorbent assays (ELISAs). OD_{450} quantification of 2741-19 binding to PfGARP ($OD_{450,\ 2741\text{-}19} = 0.88$) were over four times higher than clinically used antimalarials (OD_{450} ranges from 0.13 to 0.2; see Table 1) and statistically significant compared to controls ($p < 0.0001$). MT 2-20, DNA, lumefantrine, and piperaquine show statistically insignificant binding

to PfGARP compared to controls (see Table 1). Results are consistent with specific binding between novel compound 2741-19 and its target PfGARP. Differential binding of 2741-19 and mainstay ACT antimalarials to PfGARP is consistent with 2741-19 inhibiting *P. falciparum* growth through mechanisms of action independent from the other assessed antimalarials, satisfying a key tenant of antimalarial combination therapy.

Chapter 2: Materials and Methods

2.2.1 Antimalarial Compounds and Proteins

Stock solutions of 10 mM 2741-19, 2741-19 analog 13, MT 2-20, and DHA (Cayman Chemical) were made in DMSO (Sigma-Aldrich). These compounds were diluted with 5X coating buffer and MiliQ water to make a final 10 μM solutions in 1X coating buffer. Stock solutions of 2 mM lumefantrine (Sigma-Aldrich) and 5X buffer was diluted with MiliQ water to 10 μM lumefantrine and 1X coating buffer. Stock solutions of 2 mM piperaquine tetrahydrate tetraphosphate (Sigma-Aldrich) and 5X coating buffer was diluted with MiliQ water to 10 μM piperaquine tetrahydrate tetraphosphate and 1X coating buffer. 5X coating buffer was a carbonate-bicarbonate solution with a pH of 9.6.

2.2.2 Expression and Purification of Recombinant Proteins

A truncated immune-relevant region (PfGARP-A) of the 80 kDa target protein, PfGARP, was cloned into a bacterial expression vector encoding affinity tags to facilitate downstream purification. The construct was transformed into an *Escherichia coli* expression strain, and recombinant protein production was induced under high-density culture conditions in a controlled fermentation system. Following expression, cells were harvested and lysed by high-pressure disruption in a buffered solution containing salts, mild detergents, and low

concentrations of imidazole to maintain protein solubility and minimize nonspecific interactions. The lysate was clarified by filtration to remove insoluble debris prior to purification.

Protein purification was carried out using a multi-step chromatographic approach. Initially, the affinity-tagged protein was captured using immobilized metal affinity chromatography, exploiting the interaction between the affinity tag and a nickel-charged resin, and subsequently eluted with increasing concentrations of imidazole. The partially purified protein was then subjected to hydrophobic interaction chromatography following adjustment of salt concentration, enabling separation based on surface hydrophobicity. Further purification was achieved using anion-exchange chromatography, which separates proteins according to charge and improves overall purity. A final step using hydroxyapatite chromatography was performed to enhance protein homogeneity through interactions with calcium phosphate matrices.

Between purification steps, fractions containing the target protein were pooled and buffer conditions were adjusted to optimize performance in subsequent chromatographic separations. The purified protein was then buffer exchanged into a formulation buffer containing stabilizing agents and concentrated by ultrafiltration. The final product was lyophilized for storage, and endotoxin levels were assessed to ensure suitability for downstream applications.

2.2.3 Drug and PfGARP Binding Enzyme-Linked Immunosorbent Assays

A 96-well high-binding microplate (Greiner ref#655081) was coated with 100 µL of 10 µM drug in each well and incubated overnight at 4°C. One plate included 6 to 12 wells of 2741-19, 2741-19 analog 13, MT2-20, DHA (Cayman Chemical), lumefantrine (Sigma-Aldrich), and piperaquine (Sigma-Aldrich). Appropriate vehicle controls were made for each drug. After overnight incubation, 10X ELISA Washing Buffer (ImmunoChemistry Cat# 650) was diluted to

1X in MiliQ water. The incubated plate was washed three times with 100 μL of 1X washing buffer in each well. To prepare the blocking buffer, 5 mg of non-fat dry milk (Lab Scientific bioKEMIX Cat #M0841) was dissolved in 1X Phosphate-Buffered Saline with Tween-20 (PBST) to create a 10% solution. 80 μL of this blocking buffer was added to each well of the 96-well plate and was incubated overnight at 4°C on a shaker.

Recombinant rPfGARP-A was stored at -80°C. rPfGARP-A was diluted from 0.2 μg/μL to 12.5 μg/mL in prepared binding buffer. 5X binding buffer was made combining 0.25% Triton X-100 (Fisher BioReagents Lot 153966), 750 mM sodium chloride (Sigma Life Science Lot # SLBS5149), and 250 mM Tris-HCl. 5X binding buffer stored at 4°C and 0.2 μg/μL rPfGARP was diluted to 1X buffer and 12.5 μg/mL rPfGARP in MiliQ water. After the 96-well plate was washed thrice with 100 uL of 1X washing buffer, 80 uL of rPfGARP dilution was added to each well. The plate was incubated on a shaker at room temperature and was washed thrice with 1X washing buffer after 3 hours.

A 1:2000 dilution of perioxidase-conjugated AffiniPure Rabbit Anti-His Tag (Jackson ImmunoResearch Laboratories Code: 300-035-240) was diluted in Neptune Block (ImmunoChemistry Technologies Cat #62). 80 μL of anti-his tag solution was added to each well and incubated on a shaker at room temperature for 3 hours. After antibody incubation, the plate was washed 7 times with 100 μL of 1X washing buffer in each well. 100 μL of TMB Super Sensitive 1-Component HRP Microwell Substrate (ImmunoChemistry Technologies Cat #6329) and 100 μL Stop Solution for TMB Substrate (ImmunoChemistry Technologies Cat #6282) was added to each well before plate was absorbance OD was measured at 450 nm using a UV max kinetic microplate reader (Molecular Devices). Figure 9 depicts the well constitution at each step of this process.

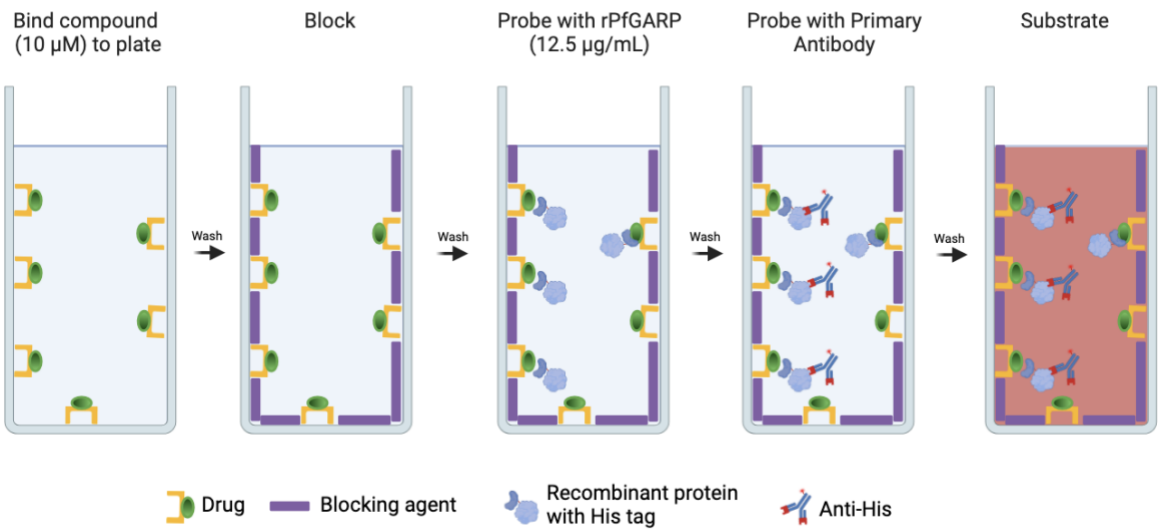

Figure 9 ELISA protocol used to assess antimalarial drug binding to PfGARP.

2.2.5 Statistical Analysis

Statistical analysis on ELISA results was carried out with a one-way analysis of variance (ANOVA) test in GraphPad Prism 10 version 10.6.1 assuming a normal Gaussian distribution. Statistically significant group variation was determined using unpaired t-tests in GraphPad Prism 10 version 10.6.1. Bar charts were generated using mean with SEM of data points. Unpaired t-tests for piperaquine were calculated separately with its no drug vehicle controls since piperaquine was the only compound in solution with water not DMSO (Appendix Figure 1). Statistical significance is considered $p < 0.05$.

Chapter 3: Results

ELISAs were employed to quantify antimalarial (i.e., DHA, lumefantrine, and piperaquine) binding to the recombinant protein PfGARP-A. 'No drug' consists of the vehicle control readings of each drug. Mean readings of 2741-19 (n = 21), 2741-19 analog 13 (n = 21), MT2-20 (n = 15), DHA (n = 15), lumefantrine (n = 15), piperaquine (n = 15), and the no drug control (n = 45) are 0.88, 0.45, 0.17, 0.20, 0.19, 0.13, and 0.21, respectively (Table 1).

Compound	(n)	Mean Reading (OD_{450} nM)	T-test to no drug control
2741-19	21	0.88	$p < 0.0001$
2741-19 analog 13	21	0.45	$p = 0.0027$
MT 2-20	15	0.17	$p = 0.2239$
DHA	15	0.20	$p = 0.4683$
Lumefantrine	15	0.19	$p = 0.2694$
Piperaquine	15	0.13	$p = 0.1857$

Table 1 Results of ELISA assays assessing antimalarial binding to rPfGARP. Data is representative of two repeated assays.

One-way ANOVA test shows statistically significant differences between drug binding readings ($p < 0.0001$). 2741-19 (n = 21; mean = 0.88) binding quantification was more than 4X greater than no drug (n = 45; mean = 0.21) binding, which was confirmed statistically significant using an unpaired two-tailed t-test ($p < 0.0001$). 2741-19 analog 13 shows some binding to rPfGARP-A and a statistically significant difference from the control ($p = 0.0027$). 2741-19 shows a statistically significant increase in binding compared to 2741-19 analog 13 ($p = 0.0030$). There is no statistically significant difference in readings between MT2-20 ($p = 0.2239$), DHA ($p = 0.4683$), lumefantrine ($p = 0.2694$), or piperaquine ($p = 0.1857$) and their appropriate 'No drug' control.

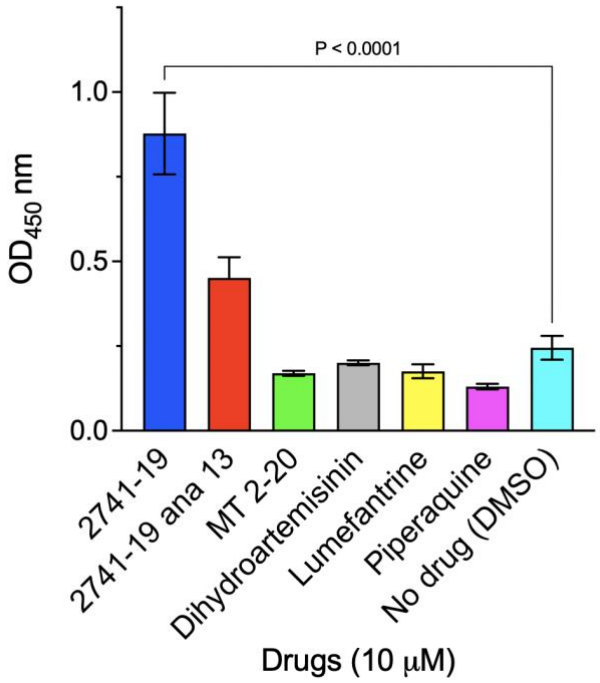

Figure 10 ELISA OD_{450} quantification of 2741-19 and antimalarial binding to rPfGARP-A. Data is representative of two repeated assays. Noise was subtracted from readings using control wells void of rPfGARP-A. Bars are representative of mean with SEM. Piperaquine vehicle control (H_20) excluded. 'No drug (DMSO)' results for piperaquine included in Appendix Figure 1.

Chapter 4: Discussion

Enzyme-linked immunosorbent assays (ELISA) were optimized and utilized to determine whether the novel compound 2741-19 has binding specificity to PfGARP compared to other antimalarial compounds. We used the recombinant protein rPfGARP-A. rPfGARP-A is the immuno-relevant subunit of the larger 80 kDa PfGARP protein identified by isolating the largest clone. Alongside 2741-19 in ELISAs, we tested two additional novel compounds (i.e., 2741-19 analog 13 and MT 2-20) that were discovered in the Kurtis Laboratory through the same library screening process described in Section 1.1.6. While MT 2-20 shows activity against parasite growth *in vivo*, 2741-19 analog 13 does not show any killing ability. We tested the clinically relevant ACT drugs, DHA, lumefantrine, and piperaquine.

Figure 10 shows rPfGARP-A binding specificity to compound 2741-19 compared to other compounds tested. 2741-19 analog 13 shows some binding to rPfGARP despite its inability to kill *P. falciparum* in growth inhibition assays. This is especially interesting result and is further evidence to suggest that binding between 2741-19 and PfGARP is an essential aspect of parasite inhibition. Binding is not seen between MT2-20, DHA, lumefantrine, or piperaquine and rPfGARP-A as determined from statistically insignificant results when compared to their respective 'No Drug' controls (Figure 10; Table 1).

Considering the clinically used compounds are known to kill *P. falciparum,* it can be concluded that is unlikely they interact with PfGARP or kill the parasite through exofacial binding with PfGARP. These results are consistent with 2741-19 binding to PfGARP in its mechanism of action and other antimalarials likely do not interact with PfGARP as an exofacial protein. As mentioned in Section 2.2.3, though lumefantrine's mechanism of action is not well characterized or understood, lack of binding to PfGARP seen in Figure 10 confirms that it is extremely unlikely that lumefantrine catalyzes parasite death or inhibits parasite growth through PfGARP binding. While piperaquine's suggested mechanism of action occurs in the digestive vacuole, lack of binding means it likely does not interact with PfGARP in an auxiliary manner.

Recent *in vivo* research on the joint effects of artemisinin combination therapy shows antagonism between the active metabolite of artemisinin, DHA, and 4-aminquinoline ACT partner drugs, chloroquine, piperaquine, and amodiaquine.[25] Additionally, they found DHA antagonism severity increased in chloroquine resistant parasite strains.[25] While DHA has a separate mechanism of action from 4-aminoquinolines, they hypothesize the interaction of 4-aminoquinolines with heme reduces the effectiveness and activity of DHA.[25] These results demonstrate the importance of partner drugs acting on separate pathways within parasite

inhibition. Compounds in combination that target intracellular and extracellular pathways of *P. falciparum* infection would be an advantageous addition to our arsenal of antimalarial combination therapies, such as 2741-19 and partner drugs that do not bind PfGARP.

While unique rPfGARP-A binding is a promising start for distinguishing the distinct mechanisms of action between 2741-19 and other antimalarials, it is not conclusive evidence, and further experimentation needs to be conducted for confirmation. Additionally, ELISAs are idealized and optimized conditions that do not reflect parasite-host physiology and cannot account for *in vivo* accessibility, affinity, membrane localization, or host-parasite interactions. Further screening with more antimalarials would be beneficial and could strengthen claims of rPfGARP-A binding specificity to 2741-19.

Further experimentation could be pursued to confirm results of 2741-19 specific binding to rPfGARP-A is also seen in rPfGARP-FL, though there is no basis to suppose results of PfGARP-FL would be different from rPfGARP-A or have different scientific implications for 2741-19 binding. Throughout all Kurtis Laboratory research with Pf-GARP, differing and consequential experimental results of PfGARP-A compared to PfGARP-FL is rare. These ELISA experiments should also be repeated with native PfGARP protein to confirm the results seen using recombinant PfGARP-A.

Chapter 5: Conclusions

ELISA assays demonstrate specific binding between 2741-19 and its target *P. falciparum* exofacial recombinant protein, PfGARP-A. These results are consistent with 2741-19 and PfGARP binding playing a crucial role in 2741-19's antimalarial mechanism of action and supports compound-protein target specificity.

Part III: 2741-19 synergizes with ACT partner drug, piperaquine, *in vitro* to kill *P. falciparum*

Abstract

Plasmodium falciparum malaria infects 300-500 million individuals and accounts for over 600,000 deaths each year with most deaths occurring in children under 5 years of age living in sub-Saharan Africa. In the past several years, morbidity and mortality due to *P. falciparum* have increased. The spread of parasites resistant to artemisinin, the mainstay of treatment, threatens to exacerbate this trend, underscoring the urgent need to identify novel antimalarial drugs. Previously, we identified a novel antimalarial small molecule drug, 2741-19, that binds with PfGARP, a malarial protein expressed on the exofacial surface of infected human erythrocytes. 2741-19 kills malaria parasites with an IC_{50} of 50 nM with no observable toxicity to mammalian cells. To forestall the development of resistance, *P. falciparum* infections are treated with artemisinin-based combination drug therapy. Key partner drugs for artemisinin in Kenya are lumefantrine and piperaquine, a 4-aminoquinoline. To assess the potential for synergy in parasite killing between 2741-19 with potential partners, lumefantrine and piperaquine, we performed *in vitro* parasite growth assays with a dose response matrix design. Synergy was quantified using four reference models including Loewe Additivity, Bliss Independence, Highest Single Agent (HSA), and Zero Interaction Potential (ZIP). In all context relevant models, 2741-19 demonstrated significant synergy with piperaquine in mediating parasite killing reflecting greater parasite killing than would be expected if the interaction were merely additive. These findings support further evaluation of 2741-19 in combination with artemisinin partner drugs as promising candidates for a next generation of antimalarial combination therapies.

Chapter 6: Materials and Methods

3.6.1 P. falciparum 3D7 Culture

The 3D7 strain of *P. falciparum* parasites were cultured *in vitro* at < 5% parasitemia and 2% hematocrit in culture medium. RPMI-1640 culture medium contained Glutamax, 25 mmol/L HEPES (Gibco Cat# 72400-047), 5% human O+ erythrocytes (Rhode Island Blood Center), 0.5% (w/v) Albumax II (Gibco Cat#11021-037), 100 μM hypoxanthine and 16 μM thymidine (Gibco Cat# 11067-030), 25 μg/mL gentamicin (Gibco Cat# 15710-064) gassed with 5% CO_2, 1% O_2, and 94% N_2 and incubated at 37°C.

3.6.2 2741-19, Artemisinin Derivatives, and ACT Partner Drugs

Piperaquine tetrahydrate tetraphosphate (Sigma-Aldrich) was dissolved in MiliQ water at 5 mg/mL to create a 2 mM stock solution stored at -80°C. Lumefantrine (Sigma-Aldrich) was dissolved in DMSO (Sigma-Aldrich) at 5 mg/mL to create a 2 mM stock solution stored at -80°C. DHA was purchased from Cayman Chemical dissolved in DMSO at 5 mg/mL. Piperaquine and lumefantrine 2 mM stock solutions were stored at -80°C and diluted with complete culture media for each assay.

3.6.3 Drug Sensitivity on Asexual Blood Stage Parasites

Initial growth inhibition assays (GIAs) were conducted with partner drugs lumefantrine and piperaquine to determine approximate IC_{50} values. Before growth inhibition assays (GIA) were plated, the 3D7 parasite culture were ring-stage synchronized twice with 5% D-Sorbitol (Aldrich-Sigma) and the culture parasitemia was maintained below 5%. GIAs were plated in a 96-well round-bottom culture-treated polystyrene plate (CELLTREAT Cat #229190). The 2 mM stocks of piperaquine and lumefantrine, were diluted in the culture medium (see Section 3.6.1) to final concentrations of 4 μM. Each drug was plated in duplicate and two-fold serial diluted across the plate. Previously synchronized ring-stage parasites were added to each well creating

final volume of 150 μL in each well with a parasitemia of 0.4%, 1% hematocrit, and drug concentrations ranging from 3.90625 nM to 2 μM. The 96-well plate was gassed in a chamber with 5% CO_2, 5% O_2, and 90% N_2 and was incubated at 37°C for 72 hours.

After the incubation, well contents were stained with 20 mM Hoescht (Thermo Scientific lot YI4017055) diluted to 4 μM solution for 30 minutes and then washed twice with 1X PBS. Parasitemia of each well was quantified using the CytoFLEX (Beckman Coulter) flow cytometer. Based on the quantified parasitemia at each plated drug concentration, the inhibitory concentration that killed 50% of parasites (IC_{50}) in culture was calculated using a non-linear 4-parameter regression in GraphPad Prism 10 version 10.6.1.

3.6.4 Dose-Response Assay Matrix Design

As described by Caser and Cech, a dose-response matrix assay design is required to comprehensively determine *in vitro* synergy. This research employs the suggested checkerboard growth inhibition assay adapted from Bellio et al. and utilizes conditions that closely resemble human physiology.[29,30] This method consists of preparing three drug dilutions of two drugs (i.e., drug A and drug B) and performing one vertical two-fold serial dilution with drug A and one horizontal serial dilution with drug B prior to plating diluted and ring-synchronized *P. falciparum* parasites. Solutions four times more concentrated than the maximum desired concentration of drug A (S_A) and four times more concentrated than the maximum desired concentration of drug B (S_B) were diluted in culture media from 2 mM stock solutions. A second dilution of drug A was made, equivalent to $2 \times S_A$, or 8 times more concentrated than the desired maximum concentration. Maximum desired concentrations of S_A and S_B were determined based on initial determinations of IC_{50} for each drug. For each maximum desired concentration of drug A and drug B, two assays were plated at the same time such that each drug was diluted vertically

from top to bottom on one plate and horizontally from right to left on the other to capture the widest range of drug concentration combinations.

As standard in *P. falciparum* GIAs, the exterior wells of the 96-well plate were not used and filled with 200 μL of media. 100 μL of S_A was plated in wells B2 to B10 and 100 μL of 2 × S_A was added to well B11. 100 μL of culture medium was added to the rest of the plate. Vertically, from top to bottom (i.e., row B to row F), the plated concentrations of drug A were two-fold serially diluted using a multichannel pipette. 100 μL of S_B was added in wells B11 to G11 and horizontally serially diluted from right to left (i.e., column 11 to column 3) using a multichannel pipette.

After the vertical dilution of S_A and horizontal dilution of S_B, there are 45 different combinations of drug A and drug B concentrations. Column 2 is exclusively varying concentrations of drug A and row G is exclusively varying concentrations of drug B from which the independent IC_{50} of each drug will be derived. There are three drug free negative control wells, G2, H2, and H3. Previously synchronized ring-stage parasites were added to each interior well creating final volume of 200 μL with a parasitemia of 0.4% and 1% hematocrit. The addition of parasites reduces the combinations of drug concentrations by half. The 96-well plate was gassed in a chamber with 5% CO_2, 5% O_2, and 90% N_2 and was incubated at 37°C for 72 hours. Parasitemia was quantified using flow cytometry (see Section 3.6.3).

3.6.5 Reference Models of Synergistic Drug Interaction

To determine synergistic drug combinations and quantify the degree of drug interaction, different reference models calculate a null hypothesis of non-interaction for given drug concentrations in combination and compare that expected value to the experimental response. Using the publicly available website SynergyFinder.org, four reference models (i.e., Bliss

Independence, Loewe Additivity, Zero-Interaction Potential (ZIP), and Highest Single-Agent (HSA)) were utilized to analyze interactions between 2741-19 and the ACT partner drugs lumefantrine and piperaquine.[31] Response at each drug concentration combination was calculated as a percent of inhibition compared to negative control wells in each plate after normalizing for flow cytometer reading noise. Synergy scores are calculated as the difference between the experimental percent inhibition and the expected response as determined by each synergy respective model.[28] Synergy scores in Synergy Finder are 'after' imputation and corrected as offered in the Synergy Finder interface. Missing experimental values are imputed based on multiple imputation by chained equations (MICE).

Bliss Independence, Loewe Additivity, and HSA are the three foundational synergy reference models that provide a basis for all models developed in the past century.[32] They are based on the following three mathematical principles respectively: Multiplicative Survival Principle (MSP), Dose-Equivalence Principle (DEP), and Highest Single-Agent (HSA).

To describe the four reference models employed, let drug 1 at dose x_1 produce a response y_1 and drug 2 at dose x_2 produce a response y_2. In the simplest examples, the Highest Single Agent (HSA) model computes expected value as the maximum of the independent drug responses. This determines synergy as the difference between the experimental response of drugs in combination and the most efficacious individual drug response:[32]

$$y_{HSA} = \max(y_1, y_2)$$

The Bliss Independence model, based on MSP, claims the probability of being unaffected by each drug is independent.[33,32] The biological interpretation of the Bliss Independence model surmises that the drugs are acting on separate pathways and responses are the result of independent events or actions.[34] The effects caused by compounds together are mutually non-

exclusive described as a combined probability and calculated as subtracting the overlap.[35] Thus, the expected response of combination of events is equal to the probability of either drug exerting their independent response, y_1 and y_2:

$$P(y_1 \cup y_2) = P(y_1) + P(y_2) - P(y_1 \cap y_2)$$

Therefore,

$$y_{BLISS} = y_1 + (1 - y_1)y_2 = \ y_1 + y_2 - y_1 \cdot y_2$$

Alternatively, the Loewe Additivity model suppose the null hypothesis of non-interaction from the DEP or 'sham-experiment', where non-interaction is the response in which 'the effect of reducing one drug's concentration can be compensated for by adding a second drug at a constant ratio.'[32] Under Loewe Additivity, drug response is mutually exclusive. When one drug can be substituted for another drug in constant proportion, the interaction is considered additive not synergistic, constituting the expected value for the Loewe Additivity model. A biological interpretation of Loewe Additivity assumes the two drugs in combination are acting on the same molecular pathway.

The Loewe Additivity model utilizes the 4-parameter log-logistic dose-response curves (i.e., y = $f_1(x)$ and y = $f_2(x)$ for drug 1 and drug 2 respectively) generated from each drug's independent responses to determine the expected response of the drugs in combination (i.e., y_{LOEWE}).[32] This model's assumed baseline is that the expected response would be the same as adding the drug to itself, $f_1(x) = \ f_2(x)$ and furthermore, $y_{LOEWE} = f(x_1 + x_2)$. The inverse of the dose response curves (i.e., $f_1^{-1}(y_{LOEWE})$ and $f_2^{-1}(y_{LOEWE})$ for drug 1 and drug 2 respectively) produces the dose responsible for the expected effect, y. This model must satisfy the following equations where E_{min} and E_{max} are the minimal and maximal effects of the drug and $m_{1,2}$ are the IC_{50}, or half maximal inhibitory concentration, of drug 1 and drug 2

respectively. $\lambda_{1,2}$ are the shape of the parameters of the dose-response curve. It assumes that dose-response curves are parallel and potency is constant:

$$\frac{x_1}{f_1^{-1}(y_{LOEWE})} + \frac{x_2}{f_2^{-1}(y_{LOEWE})} = 1$$

$$\frac{x_1}{m_1(\frac{y_{LOEWE} - E^1_{min}}{E^1_{max} - y_{LOEWE}})^{\frac{1}{\lambda_1}}} + \frac{x_2}{m_2(\frac{y_{LOEWE} - E^2_{min}}{E^2_{max} - y_{LOEWE}})^{\frac{1}{\lambda_2}}} = 1$$

The Zero-Interaction Potential (ZIP) reference model uses the dose response curves of drug responses independently to calculate an expected effect of drug 1 and drug 2 in combination under the circumstances that they act independently would not potentiate one another.[36,37] In this sense, the ZIP model is a parameterized MSP.[32] This results in an equation based on the same mathematical basis as the Bliss Independence model using probabilistic assumptions of independent events where drug responses are based on dose response curves rather than independent drug response:

$$y_{ZIP} = \frac{(\frac{x_1}{m_1})^{\lambda_1}}{(1+\frac{x_1}{m_1})^{\lambda_1}} + \frac{(\frac{x_2}{m_2})^{\lambda_2}}{(1+\frac{x_2}{m_2})^{\lambda_2}} - \frac{(\frac{x_1}{m_1})^{\lambda_1}}{(1+\frac{x_1}{m_1})^{\lambda_1}} \cdot \frac{(\frac{x_2}{m_2})^{\lambda_2}}{(1+\frac{x_2}{m_2})^{\lambda_2}}$$

Synergy scores from a specific reference model and drug concentrations are referred to using the format $S_{\text{MODEL TYPE}}$ (2741-19 concentration (nM), partner drug concentration (nM)). Percent of concentration combinations of a specific interaction designation (i.e., synergy, non-interaction, antagonism) are calculated at the number of synergy scores constituting that designation divided by the total number of concentration combinations (54 combinations for 2741-19 with lumefantrine and 100 combinations for 2741-19 with piperaquine).

Chapter 7: Results

3.7.1 P. falciparum sensitivity to ACT partner drugs

As described in Section 3.6.3, we conducted initial GIAs with 3D7 *P. falciparum* parasite strain to determine the IC_{50} values of ACT partner drugs lumefantrine and piperaquine. Lumefantrine's IC_{50} was 6.057 nM and piperaquine's IC_{50} was 16.62 nM (Figure 11). 2741-19 had an IC_{50} of 33 nM in these assays but ranges from around 30 to 80 nM in our research. These IC_{50} values were the basis of designing the matrix drug combination assays (see Section 3.6.3 and 3.6.4) and determining appropriate concentration ranges for each drug. Lumefantrine and piperaquine IC_{50} values were consistent with values stated in 3D7 growth inhibition assay literature.

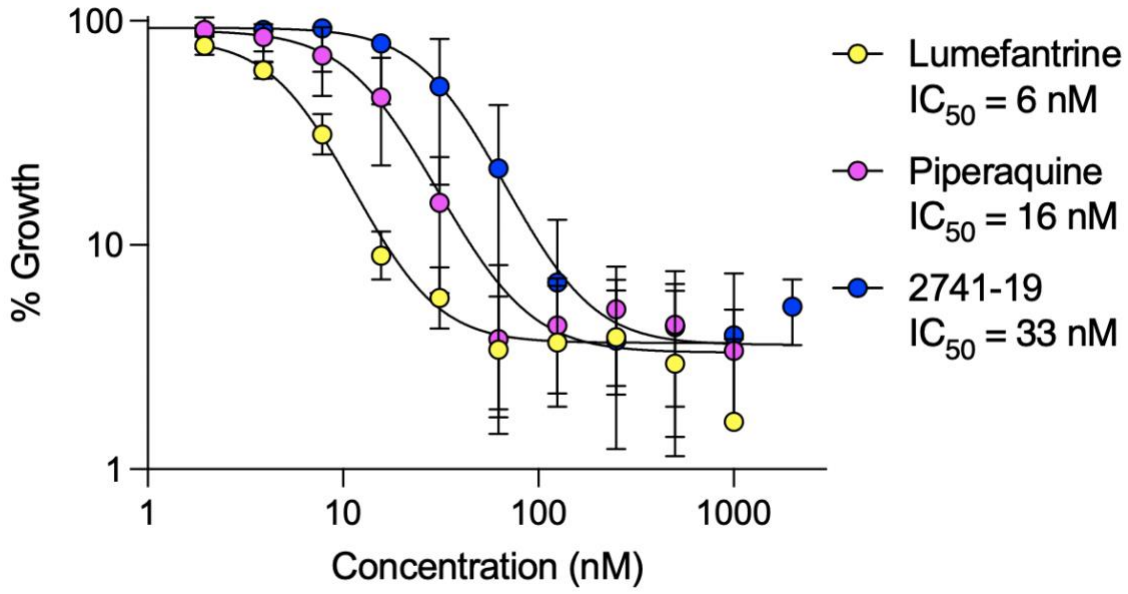

Figure 11 *In vitro* growth inhibition of 2741-19, lumefantrine, and piperaquine on 3D7 parasites. Lumefantrine and piperaquine data representative of two assays each with two replicates of each well concentration. 2741-19 dose response curve representative of 7 growth inhibition assays. Parasitemia readings were adjusted for noise using the average reading of red blood cell wells (n = 3) with equivalent hematocrit to experimental wells for each assay.

3.7.2 Novel compound 2741-19 in combination with lumefantrine

Based on IC_{50} values determined in section 3.7.1, growth inhibition assays of 2741-19 and lumefantrine were designed with concentration ranges of around 7.8 nM to 2000 nM and 3.9 nM to 125 nM respectively. 2000 nM is the standard maximum concentration used in 2741-19 GIAs. 125 nM of lumefantrine was chosen because it is about 20 times the IC_{50}. Four reference synergy models (i.e., Bliss Independence, Loewe Additivity, HSA, and ZIP) were utilized to assess synergistic drug interactions from the quantified parasitemia of each drug combination in GIAs (Figure 11). Figure 12 depicts the synergy scores of each reference model depicted in three different graphical formats. Across reference models, synergy is determined from scores greater than 10 and antagonism is determined from scores less than -10. Synergy scores between -10 and 10 are considered merely additive or non-interactive, satisfying the null hypothesis of non-interaction and failing to reject the null hypothesis.

The Bliss and ZIP reference models showed relatively little variation from the expected response of drugs in combination with maximum synergy scores of $S_{\mathrm{BLISS,\,max}}(15.625, 15.625) = 3.56$ and $S_{\mathrm{ZIP,\,max}}(31.25, 15.625) = 2.7$. This is discernable from the relatively flat three-dimensional response surface in A.1 and C.1 of Figure 12. The Bliss and HSA models share a global minimum at the same concentrations of 2741-19 and lumefantrine ($S_{\mathrm{BLISS,\,min}}(62.5, 125) = -22.78$; $S_{\mathrm{HSA,\,min}}(62.5, 125) = -19.5$). The Loewe Additivity reference model shows significant antagonism around the IC_{50} ranges of 2741-19 and lumefantrine in combination, specifically around concentrations of 15.625 to 31.25 nM of 2741-19 ($S_{LOEWE,\,min}(31.25, 3.90625) = -24.2$). Moderate to weak synergy is seen in the HSA model with a maximum score of $S_{\mathrm{HSA,\,max}}(62.5, 7.8125) = 16.57$. Synergy scores for all 2741-19 and lumefantrine concentration combinations are available in Appendix Table 1.

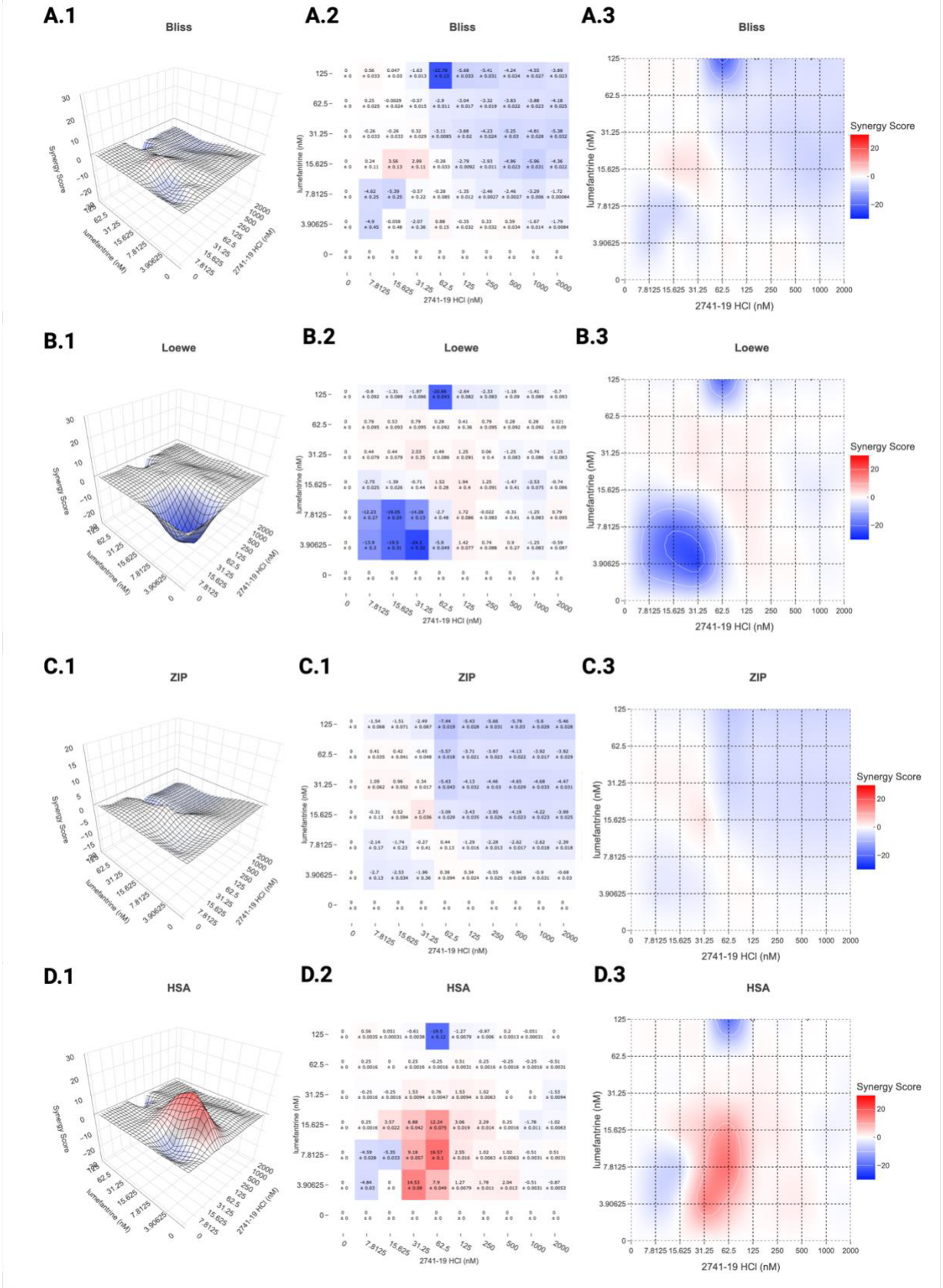
A.1
Bliss
A.2
Bliss
A.3
Bliss
B.1
Loewe
B.2
Loewe
B.3
Loewe
C.1
ZIP
C.1
ZIP
C.3
ZIP
D.1
HSA
D.2
HSA
D.3
HSA
Synergy Score
lumefantrine (nM)
2741-19 HCl (nM)
0
7.8125
15.625
31.25
62.5
125
250
500
1000
2000
3.90625

Figure 12 Synergy scores for growth inhibition assays of 2741-19 in combination with lumefantrine based on four reference models (A-D). Scores represented with three different visualizations for each reference model (1-3). Heatmaps for each model show the calculated synergy score and standard deviation.

3.7.3 Novel compound 2741-19 in combination with piperaquine

The same four synergy models used in Section 3.7.2 were used to assess drug interactions of 2741-19 and piperaquine. Figure 13 depicts the synergy scores of each reference model in three different graphical formats. Based on IC_{50} values determined in Section 3.6.1, the growth inhibition assays of 2741-19 and piperaquine were designed with concentration ranges of around 0.98 nM to 500 nM and 0.39 nM to 200 nM respectively. Synergy scores greater than 10 indicate synergistic drug interactions and below -10 constitute antagonistic drug interactions. Scores between -10 and 10 are consistent with an additive or non-interactive drug interactions.

2741-19 and piperaquine show significant synergy and no antagonism in the Bliss Independence reference model as defined by synergy scores exceeding 10 and none below the antagonism threshold of -10. Bliss Independence synergy scores for 2741-19 and piperaquine have a maximum score of $S_{\text{BLISS, max}}(31.25, 1.5625) = 26.98$ and a minimum of $S_{\text{BLISS, min}}(62.5, 6.25) = -8.19$. Generally, this is observed in the HSA and ZIP reference model with maximum scores of $S_{\text{HSA, max}}(62.5, 1.5625) = 22.55$ and $S_{\text{ZIP, max}}(31.25, 1.5625) = 21.66$ and minimum scores of $S_{\text{HSA, min}}(0.976, 6.25) = -7.56$ and $S_{\text{ZIP, min}}(0.976, 0.39) = -13.52$. Loewe Additivity for 2741-19 and piperaquine shows specific concentration combinations peaks of synergy ($S_{LOEWE}(31.25, 0.78125) = 15.48$) and antagonism ($S_{LOEWE}(31.25, 6.25) = -25.04$). Synergy scores for all 2741-19 and piperaquine concentration combinations are available in Appendix Table 2.

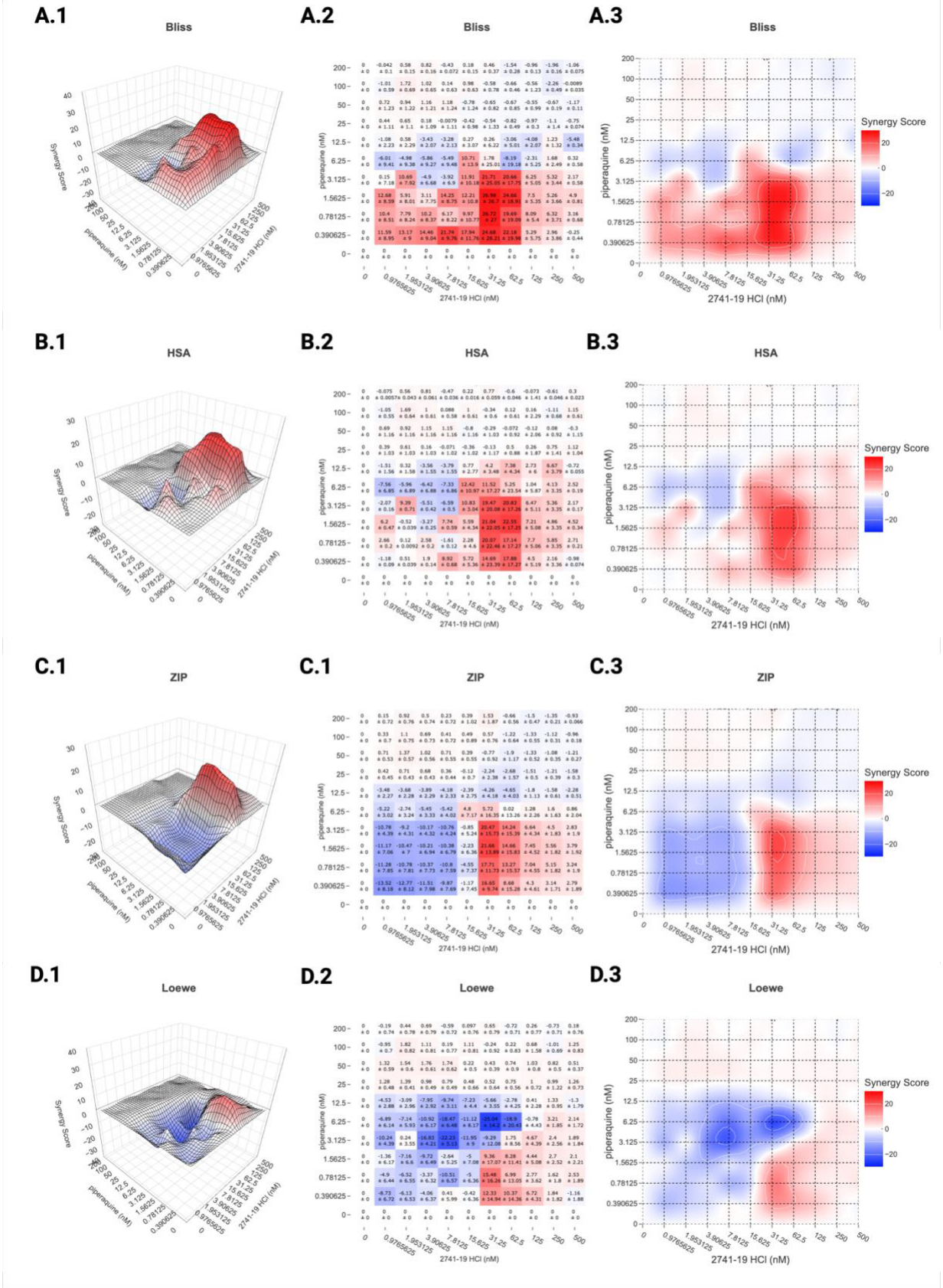
A.1
Bliss
A.2
Bliss
A.3
Bliss
B.1
HSA
B.2
HSA
B.3
HSA
C.1
ZIP
C.1
ZIP
C.3
ZIP
D.1
Loewe
D.2
Loewe
D.3
Loewe
Synergy Score
piperaquine (nM)
2741-19 HCl (nM)

Figure 13 Synergy scores for growth inhibition assays of 2741-19 in combination with piperaquine based on four reference models (A-D). Scores represented with three different visualizations for each reference model (1-3). Heatmaps for each model show the calculated synergy score and standard deviation.

Chapter 8: Discussion

In Chapter 6, *in vitro* synergy of 2741-19 and antimalarial partner drugs was assessed to determine if there could be additional benefits of using 2741-19 as a combination therapy beyond extended half-life and unique mechanisms of parasite killing to prevent drug resistance events. The goal of using drug synergy models in this research is to prioritize potential partner drugs for novel compound 2741-19. We demonstrated strong *in vitro* synergy between 2741-19 and piperaquine but did not see the same beneficial enhanced killing in combinations of 2741-19 and lumefantrine. Therapeutic antimalarial drug pairings with synergistic interactions could be beneficial in increasing treatment efficacy and reducing drug dosing, potentially reducing the risk of side-effects.[31]

In synergy models, the null hypothesis assumes non-interaction of the drugs in combination. Synergy models differ in their approach to determine the null hypothesis of non-interaction, resulting in varying expected values representing non-interaction and potentially divergent synergy results in different models. Synergistic drug interaction is determined as significant positive deviation from a null hypothesis of non-interaction, typically quantified as synergy scores greater than 10. Drug antagonism is quantified as synergy scores less than -10, which constitutes significant negative deviation from the null hypothesis of non-interaction. In general, synergy models are built on one of three underlying mathematical principles: Dose-Equivalence Principle (DEP), Multiplicative Survival Principle (MSP), or Highest-Single Agent (HSA).[32] Loewe Additivity is built on the DEP and parameterizing assumptions of the MSP result in the ZIP synergy model.[32] Bliss Independence is based on notions of the MSP. As

mentioned in Section 3.6.5, four synergy reference models were utilized, specifically Bliss Independence, Loewe Additivity, HSA, and ZIP.

Since drug synergy models were proposed in the early 20th-century, there has been significant debate about determining the 'best' synergy model, leading to the Saariselkä Agreement in 1992.[38,34] Attendees resolved that there is not a single universal synergy model.[34] Differences in synergy model results based on whether the null hypothesis of non-interaction is predicated on the DEP or MSP are to be expected based on the biological interactions of drugs and are both theoretically justified.[34] While in practice there may be debate on inconsistencies across models, this is inherent in the different assumptions the models are built on.[34] Approaches to reconciling differences in synergy reference model results span both determining consensus synergy across models or selecting synergy reference models in the context of the data being analyzed.[37,39]

In combination with novel compound 2741-19, we looked at the two most popular ACT partner drugs prescribed in Africa, lumefantrine and piperaquine. Growth inhibition assays were used to quantify *P. falciparum* killing of different drug concentration combinations (see Sections 3.6.3 and 3.6.4). Contradictory or varying conclusions of synergy in different synergy reference models is a commonly cited critique of drug synergy assessments but stems from the variation of approaches to calculating non-interaction in reference models.[32]

3.8.1 Synergy assessment of 2741-19 and lumefantrine

We conclude 2741-19 and lumefantrine do not show enhanced or decreased drug-drug interactions based on synergy results of non-interaction in the ZIP and Bliss models and inconsistent conclusions in the HSA and Loewe models. Concentration specific synergy between 2741-19 and lumefantrine was shown in the most basic reference model, HSA, with around 5%

of scores exceeding the threshold of 10 constituting drug synergy. Synergistic scores in the HSA model are seen from 31.25 to 62.5 nM of 2741-19, almost double the IC_{50} of 2741-19 (IC_{50} = 33 nM), and from 3.9 to 15.625 nM of lumefantrine (IC_{50} = 6 nM). This is an interesting range to see synergy considered we would expect almost if not complete inhibition in this range. The opposite interaction of antagonism in this range in the Loewe model exemplifies the inconsistencies that can occur across synergy models and the dose response sensitivity that can occur around a compound's IC_{50}.

Antagonism was demonstrated in the Loewe Additivity model (Figure 12.B) with almost 13% of concentration combinations resulting in a synergy score less than -10 because of lower-than-expected parasite killing of the drugs in combination. These antagonistic combinations are mostly concentrated under 31.25 nM of 2741-19 and under 7.8125 nM of lumefantrine. Considering that 2741-19's IC_{50} = 33 nM and lumefantrine's IC_{50} = 6 nM, this region is where we would expect to see the most sensitivity to non-linear dose response behavior. This is clear from the opposite synergistic response in this range seen in the HSA model, weakening the claim of either model for an interaction beyond additive or non-interaction. With the mechanistic insights gleaned from Part II, it is expected that the Loewe Additivity reference model would show the lowest synergy scores since it is theoretically incompatible with expected biological mechanistic assumptions of the model. Namely, we do not expect 2741-19 to work on the same biological pathways as lumefantrine and any enhanced response would likely be the result of an independent pathway incorporating PfGARP binding.

With almost all synergy scores between -10 and 10 in Bliss and ZIP models, 2741-19 and lumefantrine in combination showed indifferent interaction. The Bliss and ZIP reference models (Figure 12.A and 12.C) result in flat synergy surfaces, indicating no interaction above or below

the expected response in those models. Apart from one trough in the Bliss Independence model ($S_{BLISS,\ min}$ (62.5, 125) = -24.2), all synergy scores for these models are between -10 and 10. With the lack of standardization in drug synergy assessment,[32] often a view of consensus synergy, where multiple models point towards the same type of drug interaction, is most compelling.[37]

The results of 2741-19 in combination with lumefantrine indicate a consensus of non-interaction based on the Bliss and ZIP models. Opposite interactions seen in the HSA and Loewe models at specific combination concentrations weaken the claim of either model beyond non-interaction. Inconsistent results across multiple synergy models are likely indicative of no drug interaction enhancing the expected response of the compounds in combination. Further research could consider using lower concentrations of 2741-19 and lumefantrine to achieve a more granular synergy assessment in the IC_{50} range.

There is one significant antagonistic synergy score present in the Bliss, Loewe, and HSA reference models at 62.5 nM of 2741-19 and 125 nM of lumefantrine (S_{BLISS} = -24.2; S_{LOEWE} = -20.86; S_{HSA} = -19.5) resulting from data imputation. This minimum is not representative of a true antagonistic interaction or experimental results. The imputed growth inhibition of these drug concentrations in combination is 75.74% (Appendix Figure 2), which is biologically unlikely to occur since this concentration range is over 20 times higher than the IC_{50} of lumefantrine and about double the IC_{50} of 2741-19 in these assays. If this concentration combination were experimentally tested, it would result in essentially 100% growth inhibition, similar to the local mean of growth inhibition (95.54%) in the lumefantrine concentration range of 31.25 to 125 nM. It was visually confirmed on CellaVision that there are no parasites present at this concentration. This antagonism is not seen in experimental values of other lumefantrine and 2741-19 combination assays performed or other combinations of 125 nM lumefantrine. Since it is at the

highest bounds of drug concentration where we see complete killing, imputed values are inconsequential to the overall interpretation of synergy scores. Future assays could be designed to have true experimental values for these concentration combinations that are otherwise imputed.

3.8.2 Synergy assessment of 2741-19 and piperaquine

Overall, we conclude *in vitro* synergistic interaction between 2741-19 and piperaquine. Seen in Figure 13, 2741-19 and piperaquine together showed significant synergistic activity in the Bliss Independence and HSA reference models. In all reference models, scores around 0 at concentrations above 25 nM of piperaquine are expected considering this range reaches double the IC_{50} concentration of piperaquine (16 nM) and thus the expected response is near 100% parasite growth inhibition, which does not leave room for a higher effect that would constitute synergy.

Using the standard synergy designation of for calculated scores greater than 10, 21% of concentration combinations for 2741-19 and piperaquine in the Bliss Independence model are synergistic. As described in Section 3.8.1, the most sensitive dose-response range is around the IC_{50}. When we consider scores below 62.5 nM 2741-19 and below 50 nM piperaquine, a range that accounts for about 2 times IC_{50} values, we see around 38% of concentration combinations are synergistic with another 7% of combinations trending towards synergy ($5 < S_{BLISS} < 10$) and 23% in this range non-interactive, but greater than 0 ($0 < S_{BLISS} < 5$). This breakdown is relevant in understanding the spatial distribution of synergy seen in the Bliss reference model. Specifically, regions of considerably high synergy are surrounded by positively trending synergy scores (Figure 12.A.2), confirming an overall synergistic interpretation. Importantly, there are no antagonistic combinations in the Bliss Independence model ($S_{BLISS,min}$ (62.5, 6.25) = -8.19 > -

10). Given the results and interpretation of 2741-19 binding in Part II, highest synergy scores in the Bliss Independence model are consistent with the mechanistic context of 2741-19 and piperaquine likely having distinct mechanisms of action on *P. falciparum* parasites.

A moderate amount of significant synergy ($S_{HSA} > 15$) is also seen in the HSA reference model with 11% of concentration combinations exceeding the synergy score cutoff of 10. The HSA model shows a similar, but less pronounced spatial pattern of significant synergy and additive regions trending towards synergy in the IC_{50} zone of both compounds (Figure 13.B). Similar to the Bliss Independence model, the HSA reference model does not show any antagonistic interactions ($S_{HSA, min}(0.977, 6.25) = -7.56$). Consensus of synergy interpretations between multiple reference models, Bliss Independence and HSA, strengthens the overall claim of synergistic interactions between 2741-19 and piperaquine.

The ZIP reference model, like the Bliss Independence model, assumes compounds act independently, and similar to the Loewe Additivity model, use the dose-response curve of each individual compound to determine expected effect at a given combination concentration.[36] Implicit in these assumptions are that potency of drugs is constant and not affected by the other compound once in combination and that the dose-response curves are parallel.[36] Biologically and in practice, both of these assumptions are most often exceptional cases than the rule.[40]

The ZIP reference model shows both regions of antagonism and synergy below piperaquine concentrations of 6.25 nM and across all 2741-19 concentrations tested. The stark shift from antagonistic to synergistic regions around 2741-19 concentrations of 15.625 nM in the ZIP models suggests an overall limitation of the ZIP model's reliance on dose-response model fitting. This region of antagonism to synergism directly correlates to the growth inhibition achieved by the compounds in combination (Appendix Figure 3). Namely, at 3.125 nM and

under of piperaquine and from 15.625 nM to 31.25 nM of 2741-19, percent inhibition increases at least doubles, compared to around a 5X increase in piperaquine growth inhibition from 6.25 to 12.5 nM. Here, we can see potencies that result in non-parallel dose-response curves, violating the first assumption of ZIP model fitting. These aspects of the specific dose-response curves generated from 2741-19 and piperaquine make the ZIP model an unreliable reference for determining drug interactions.

In Figure 13.D, 2741-19 and piperaquine showed moderate synergy in the Loewe Additivity reference model around the IC_{50} concentration of 2741-19 (31.25 nM) and low concentrations of piperaquine, but this only accounts for around 3% of concentration combinations. The majority (87%) of concentration combinations were indifferent to synergy or antagonism. The plurality (10%) of all synergy scores was antagonistic. Antagonism is seen in the most dose-response sensitive concentration range around the IC_{50} ranges of both compounds (Figure 13.D). Overall, the assumptions of the Loewe Additivity model are not well aligned with our biological understanding of how 2741-19 and piperaquine inhibit *P. falciparum* growth, making it an unreliable reference model for determining drug-drug interaction. It is notable, however, that despite the base assumptions of DEP and Loewe Additivity contradicting the mechanistic context of 2741-19 and piperaquine, we still see synergistic peaks using this model. Presence of these peaks in the Loewe model supports the relevant *in vitro* synergy seen between 2741-19 and piperaquine in the Bliss and HSA models. These enhanced interactions between 2741-19 and piperaquine could potentially be leveraged for clinical therapeutic benefit.

Since inconsistencies in synergy scores across models is common based on the inherent differences in expected response calculation of the reference models, it is particularly striking when there is consistency on synergistic assessment in multiple models, as seen in the case of

2741-19 and piperaquine. The highest synergy scores are seen in the IC_{50} range of 2741-19 and below the IC_{50} of piperaquine, consistent with expectations of dose-response sensitivity.

3.8.3 Limitations and future research

In vitro assessment of any drug will not directly correlate to *in vivo* drug effects, highlighting a prominent limitation of this research and many *in vitro* models. To understand this better, further experimentation should be conducted with drug combinations *in vivo*, specifically between 2741-19 and piperaquine based on their demonstrated synergistic potential. Prior research from Taneja et al. examined a novel antimalarial compound in combination with lumefantrine and piperaquine with *in vivo* PK studies in murine models.[41] Their results showed a negative impact on the half-life of piperaquine when used alongside their novel compound.[41] Given the described *in vitro* benefits of 2741-19 and piperaquine, it is important to conduct *in vivo* studies to ascertain whether there is a pharmacokinetic interaction between 2741-19 and piperaquine that would outweigh the benefits of synergistic parasite killing.

Additionally, GIAs assessing synergy in this research were conducted on ring-stage synchronized 3D7 parasites over a 72-hour period (see Section 3.6.3). Ongoing research in the Kurtis Lab suggests that *P. falciparum* trophozoite stage parasites are most sensitive to 2741-19, which is consistent with the appearance and proliferation of PfGARP on the erythrocytic surface during trophozoite development.[27] Experimentation with GIAs on trophozoite-stage synchronized parasites could elucidate synergistic interactions when 2741-19 will presumably have a more potent effect. Additionally, *in vitro* assays considering compounds with vastly different half-lives can be difficult to translate clinically, which provides additional opportunity to confirm these interactions with pulsing assays that aim to mimic the effects of *in vivo* treatment.[25]

Chapter 9: Conclusions

Based on differential 2741-19 binding to rPfGARP results compared to other antimalarials described in Part II, the mechanism of action of 2741-19 satisfies ACT partner drug tenants of distinct antimalarial killing pathways making it is plausible therapeutic option in combination with lumefantrine or piperaquine. These mechanistic findings are consistent with the synergistic *in vitro* findings of highest synergy between 2741-19 and piperaquine in the Bliss Independence reference model. We successfully demonstrated consistent synergistic scores across all utilized synergy models confirms *in vitro* synergy between the novel compound 2741-19 and the 4-aminoquinoline piperaquine. This makes 2741-19 and piperaquine a strong combination therapy for further development. Inconsistent synergy scores across reference models for 2741-19 in combination with lumefantrine demonstrates no beneficial *in vitro* interactions of 2741-19 and lumefantrine.

Bibliography

1. WHO. Malaria. World Health Organization. December 11, 2025. Accessed January 21, 2026. https://www.who.int/news-room/fact-sheets/detail/malaria

2. Cowman AF, Healer J, Marapana D, Marsh K. Malaria: Biology and Disease. *Cell*. 2016;167(3):610-624. doi:10.1016/j.cell.2016.07.055

3. Drugs I of M (US) C on the E of A, Arrow KJ, Panosian C, Gelband H. The Parasite, the Mosquito, and the Disease. In: *Saving Lives, Buying Time: Economics of Malaria Drugs in an Age of Resistance*. National Academies Press (US); 2004. Accessed March 27, 2026. https://www.ncbi.nlm.nih.gov/books/NBK215619/

4. Siqueira-Neto JL, Wicht KJ, Chibale K, Burrows JN, Fidock DA, Winzeler EA. Antimalarial drug discovery: progress and approaches. *Nat Rev Drug Discov*. 2023;22(10):807-826. doi:10.1038/s41573-023-00772-9

5. Kuehn A, Pradel G. The coming-out of malaria gametocytes. *J Biomed Biotechnol*. 2010;2010:976827. doi:10.1155/2010/976827

6. Okombo J, Fidock DA. Towards next-generation treatment options to combat Plasmodium falciparum malaria. *Nat Rev Microbiol*. 2025;23(3):178-191. doi:10.1038/s41579-024-01099-x

7. CDC. Clinical Features of Malaria. Malaria. May 9, 2024. Accessed January 21, 2026. https://www.cdc.gov/malaria/hcp/clinical-features/index.html

8. Share of the population infected with malaria each year. Our World in Data. Accessed April 30, 2026. https://ourworldindata.org/grapher/share-of-the-population-with-malaria

9. Roser M, Ritchie H. Malaria. *Our World Data*. Published online November 20, 2015. Accessed January 21, 2026. https://ourworldindata.org/malaria

10. Blasco B, Leroy D, Fidock DA. Antimalarial drug resistance: linking Plasmodium falciparum parasite biology to the clinic. *Nat Med*. 2017;23(8):917-928. doi:10.1038/nm.4381

11. Rosenthal PJ, Asua V, Conrad MD. Emergence, transmission dynamics and mechanisms of artemisinin partial resistance in malaria parasites in Africa. *Nat Rev Microbiol*. 2024;22(6):373-384. doi:10.1038/s41579-024-01008-2

12. Hallare J, Gerriets V. Elimination Half-Life of Drugs. In: *StatPearls [Internet]*. StatPearls Publishing; 2025. Accessed March 27, 2026. https://www.ncbi.nlm.nih.gov/sites/books/NBK554498/

13. de Vries PJ, Dien TK. Clinical Pharmacology and Therapeutic Potential of Artemisinin and its Derivatives in the Treatment of Malaria. *Drugs*. 1996;52(6):818-836. doi:10.2165/00003495-199652060-00004

14. WHO. *World Malaria Report 2025: Addressing the Threat of Antimalarial Drug Resistance*. 2025. Accessed January 21, 2026. https://www.who.int/teams/global-malaria-programme/reports/world-malaria-report-2025

15. Rosenthal PJ, Asua V, Bailey JA, et al. The emergence of artemisinin partial resistance in Africa: how do we respond? *Lancet Infect Dis*. 2024;24(9):e591-e600. doi:10.1016/S1473-3099(24)00141-5

16. Djimdé A, Lefèvre G. Understanding the pharmacokinetics of Coartem. *Malar J*. 2009;8 Suppl 1(Suppl 1):S4. doi:10.1186/1475-2875-8-S1-S4

17. Tarning Joel, Lindegårdh Niklas, Annerberg Anna, et al. Pitfalls in Estimating Piperaquine Elimination. *Antimicrob Agents Chemother*. 2005;49(12):5127-5128. doi:10.1128/aac.49.12.5127-5128.2005

18. MoH. National Guidelines for Diagnosis and Treatment and Prevention of Malaria for Health Workers. *Natl Malar Control Programme*. Published online 2016.

19. Amin AA, Zurovac D, Kangwana BB, et al. The challenges of changing national malaria drug policy to artemisinin-based combinations in Kenya. *Malar J*. 2007;6(1):72. doi:10.1186/1475-2875-6-72

20. Fançony C, Fortes-Gabriel E, Zage F, et al. Artemether-Lumefantrine Treatment Selects Plasmodium falciparum Multidrug Resistance 1 (pfmdr1) Increased Copy Number Among African Malaria Infections. *J Infect Dis*. 2025;231(6):e1119-e1128. doi:10.1093/infdis/jiaf155

21. Pernaute-Lau L, Recker M, Tékété M, et al. Decreased dihydroartemisinin-piperaquine protection against recurrent malaria associated with Plasmodium falciparum plasmepsin 3 copy number variation in Africa. *Nat Commun*. 2025;16(1):2680. doi:10.1038/s41467-025-57726-5

22. Lenharo M. First new type of malaria treatment in decades shows promise against drug resistance. *Nature*. 2025;647(8091):830-830. doi:10.1038/d41586-025-03690-5

23. Zhang S, Gerhard GS. Heme activates artemisinin more efficiently than hemin, inorganic iron, or hemoglobin. *Bioorg Med Chem*. 2008;16(16):7853-7861. doi:10.1016/j.bmc.2008.02.034

24. Wang J, Zhang CJ, Chia WN, et al. Haem-activated promiscuous targeting of artemisinin in Plasmodium falciparum. *Nat Commun*. 2015;6(1):10111. doi:10.1038/ncomms10111

25. Rosenthal M, Goldberg DE. 4-Aminoquinolines block heme iron reactivity and interfere with artemisinin action. Soldati-Favre D, ed. *eLife*. 2026;14:RP108976. doi:10.7554/eLife.108976

26. Kokwaro G, Mwai L, Nzila A. Artemether/lumefantrine in the treatment of uncomplicated falciparum malaria. *Expert Opin Pharmacother*. 2007;8(1):75-94. doi:10.1517/14656566.8.1.75

27. Raj DK, Das Mohapatra A, Jnawali A, et al. Anti-PfGARP activates programmed cell death of parasites and reduces severe malaria. *Nature*. 2020;582(7810):104-108. doi:10.1038/s41586-020-2220-1

28. Rojrung R, Kuamsab N, Putaporntip C, Jongwutiwes S. Analysis of sequence diversity in Plasmodium falciparum glutamic acid-rich protein (PfGARP), an asexual blood stage vaccine candidate. *Sci Rep*. 2023;13(1):3951. doi:10.1038/s41598-023-30975-4

29. K. Caesar L, B. Cech N. Synergy and antagonism in natural product extracts: when 1 + 1 does not equal 2. *Nat Prod Rep*. 2019;36(6):869-888. doi:10.1039/C9NP00011A

30. Bellio P, Fagnani L, Nazzicone L, Celenza G. New and simplified method for drug combination studies by checkerboard assay. *MethodsX*. 2021;8:101543. doi:10.1016/j.mex.2021.101543

31. Ianevski A, Giri AK, Aittokallio T. SynergyFinder 2.0: visual analytics of multi-drug combination synergies. *Nucleic Acids Res*. 2020;48(W1):W488-W493. doi:10.1093/nar/gkaa216

32. Meyer CT, Wooten DJ, Lopez CF, Quaranta V. Charting the Fragmented Landscape of Drug Synergy. *Trends Pharmacol Sci*. 2020;41(4):266-280. doi:10.1016/j.tips.2020.01.011

33. BLISS CI. THE TOXICITY OF POISONS APPLIED JOINTLY. *Ann Appl Biol*. 1939;26(3):585-615. doi:10.1111/j.1744-7348.1939.tb06990.x

34. Tang J, Wennerberg K, Aittokallio T. What is synergy? The Saariselkä agreement revisited. *Front Pharmacol*. 2015;6. doi:10.3389/fphar.2015.00181

35. Schindler M. Theory of synergistic effects: Hill-type response surfaces as 'null-interaction' models for mixtures. *Theor Biol Med Model*. 2017;14(1):15. doi:10.1186/s12976-017-0060-y

36. Yadav B, Wennerberg K, Aittokallio T, Tang J. Searching for Drug Synergy in Complex Dose–Response Landscapes Using an Interaction Potency Model. *Comput Struct Biotechnol J*. 2015;13:504-513. doi:10.1016/j.csbj.2015.09.001

37. Ianevski A, Giri AK, Aittokallio T. SynergyFinder 3.0: an interactive analysis and consensus interpretation of multi-drug synergies across multiple samples. *Nucleic Acids Res*. 2022;50(W1):W739-W743. doi:10.1093/nar/gkac382

38. Greco W, Unkelbach HD, Pöch G, Sühnel J, Kundi M, Bödeker W. Consensus on concepts and terminology for combined-action assessment: The Saariselkä agreement. *Arch Complex Env Stud*. 1992;4:65-69.

39. Vlot AHC, Aniceto N, Menden MP, Ulrich-Merzenich G, Bender A. Applying synergy metrics to combination screening data: agreements, disagreements and pitfalls. *Drug Discov Today*. 2019;24(12):2286-2298. doi:10.1016/j.drudis.2019.09.002

40. Roell KR, Reif DM, Motsinger-Reif AA. An Introduction to Terminology and Methodology of Chemical Synergy—Perspectives from Across Disciplines. *Front Pharmacol*. 2017;8. doi:10.3389/fphar.2017.00158

41. Taneja I, Raju KSR, Singh SP, Wahajuddin M. Assessment of pharmacokinetic compatibility of short acting CDRI candidate trioxane derivative, 99–411, with long acting prescription antimalarials, lumefantrine and piperaquine. *Sci Rep*. 2015;5(1):17264. doi:10.1038/srep17264

Appendix Figures

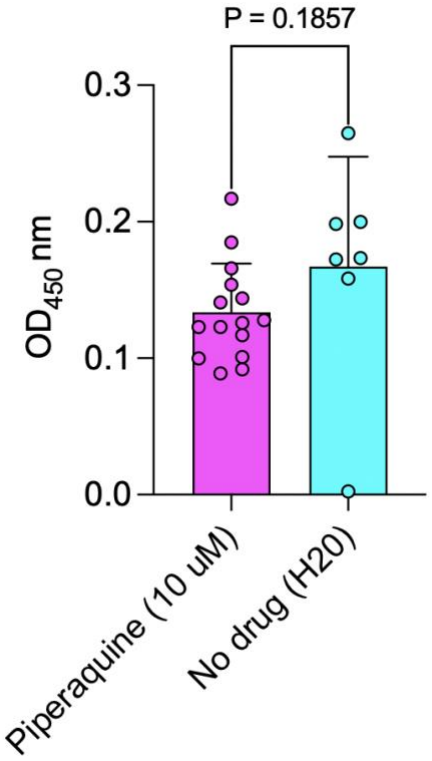

Appendix Figure 1: ELISA readings of piperaquine tetrahydrate tetraphosphate binding and H_20 vehicle control with PfGARP.

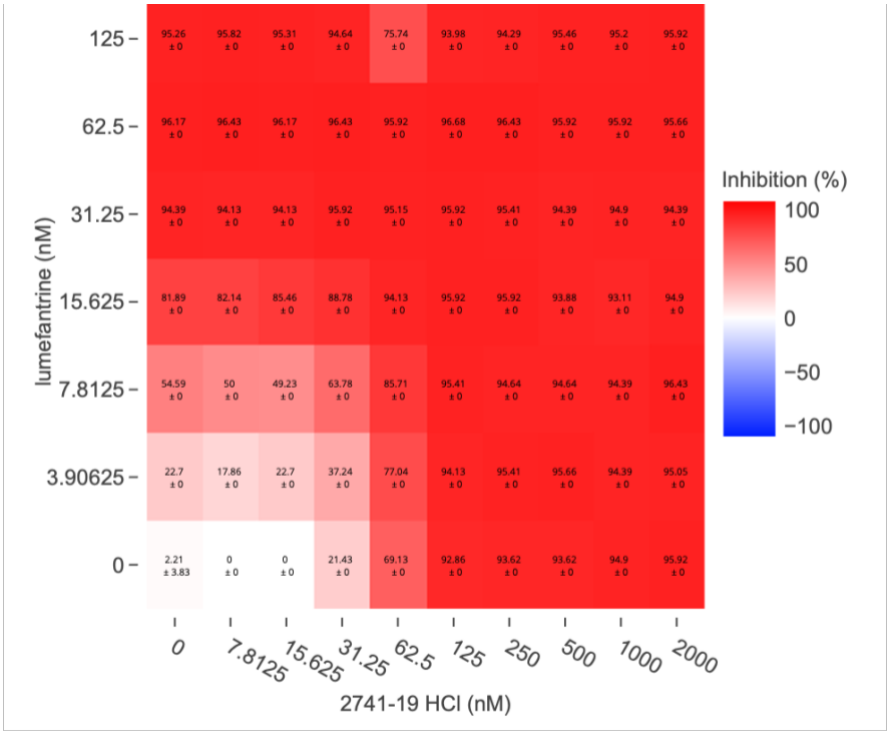

Appendix Figure 2: Dose-response heatmap of 2741-19 in combination with lumefantrine. Standard deviation shown for each concentration combination. Missing values imputed.

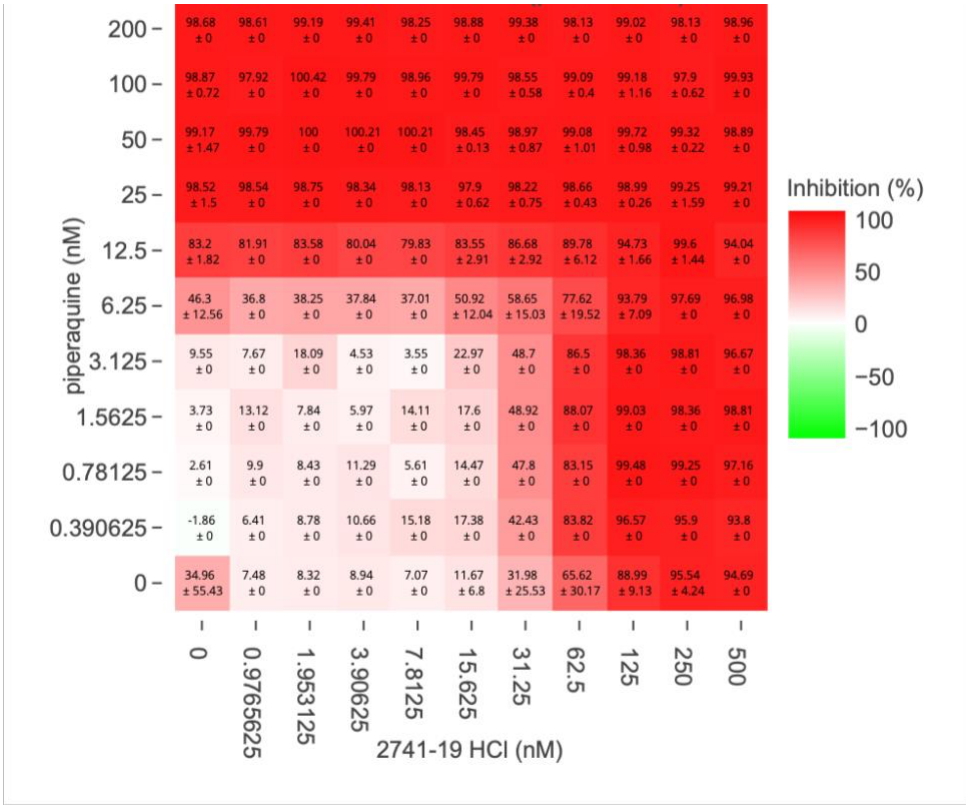

Appendix Figure 3: Dose-response heatmap of 2741-19 in combination with piperaquine. Standard deviation shown for each concentration combination. Missing values imputed.

Appendix Tables

drug 1	drug2	conc 1	conc 2	ZIP_ fit	ZIP_ ref	ZIP_syn ergy	HSA_ ref	HSA_syn ergy	Loewe _ref	Loewe_syn ergy	Bliss_ ref	Bliss_syn ergy
2741-19	lumefantrine	0	62.50	96.17	96.17	0.00	96.17	0.00	96.17	0.00	96.17	0.00
2741-19	lumefantrine	7.8125	62.50	96.38	95.36	1.02	96.17	0.26	95.88	0.54	95.44	0.99
2741-19	lumefantrine	15.625	62.50	96.42	95.55	0.87	96.17	0.00	95.88	0.29	95.63	0.55
2741-19	lumefantrine	31.25	62.50	96.23	96.67	-0.45	96.17	0.26	95.88	0.54	96.99	-0.56
2741-19	lumefantrine	62.5	62.50	93.16	98.83	-5.67	96.17	-0.26	95.88	0.03	98.82	-2.90
2741-19	lumefantrine	125	62.50	95.94	99.65	-3.71	96.17	0.51	95.99	0.70	99.73	-3.04
2741-19	lumefantrine	250	62.50	95.80	99.77	-3.97	96.17	0.26	95.88	0.54	99.76	-3.33
2741-19	lumefantrine	500	62.50	95.65	99.78	-4.13	96.17	-0.26	95.88	0.03	99.76	-3.84
2741-19	lumefantrine	1000	62.50	95.86	99.78	-3.92	96.17	-0.26	95.88	0.03	99.80	-3.89

2741-19	lumefantrine	2000	62.50	95.83	99.78	-3.95	96.17	-0.51	95.88	-0.22	99.84	-4.18
2741-19	lumefantrine	0	125.00	95.26	95.26	0.00	95.26	0.00	95.26	0.00	95.26	0.00
2741-19	lumefantrine	7.8125	125.00	95.33	96.29	-0.96	95.26	0.56	96.55	-0.73	94.35	1.47
2741-19	lumefantrine	15.625	125.00	95.31	96.44	-1.13	95.26	0.05	96.55	-1.24	94.58	0.73
2741-19	lumefantrine	31.25	125.00	94.68	97.34	-2.66	95.26	-0.61	96.55	-1.91	96.27	-1.63
2741-19	lumefantrine	62.5	125.00	91.48	99.06	-7.58	95.26	-19.51	96.55	-20.81	98.54	-22.79
2741-19	lumefantrine	125	125.00	94.26	99.72	-5.46	95.26	-1.28	96.55	-2.57	99.66	-5.68
2741-19	lumefantrine	250	125.00	94.14	99.81	-5.68	95.26	-0.97	96.55	-2.26	99.70	-5.41
2741-19	lumefantrine	500	125.00	94.02	99.83	-5.80	95.26	0.20	96.55	-1.09	99.70	-4.24
2741-19	lumefantrine	1000	125.00	94.21	99.83	-5.62	95.26	-0.05	96.55	-1.35	99.76	-4.55
2741-19	lumefantrine	2000	125.00	94.34	99.83	-5.49	95.92	0.00	96.55	-0.63	99.81	-3.89
2741-19	lumefantrine	0	31.25	94.39	94.39	0.00	94.39	0.00	94.39	0.00	94.39	0.00
2741-19	lumefantrine	7.8125	31.25	93.74	91.81	1.94	94.39	-0.26	93.18	0.95	93.31	0.82
2741-19	lumefantrine	15.625	31.25	93.85	92.14	1.71	94.39	-0.26	93.52	0.61	93.59	0.55
2741-19	lumefantrine	31.25	31.25	94.84	94.12	0.71	94.39	1.53	93.75	2.17	95.59	0.33
2741-19	lumefantrine	62.5	31.25	92.47	97.94	-5.46	94.39	0.77	93.97	1.18	98.27	-3.11
2741-19	lumefantrine	125	31.25	95.28	99.38	-4.09	94.39	1.53	94.76	1.16	99.60	-3.68
2741-19	lumefantrine	250	31.25	95.16	99.59	-4.43	94.39	1.02	94.87	0.54	99.64	-4.23
2741-19	lumefantrine	500	31.25	94.99	99.61	-4.63	94.39	0.00	95.09	-0.70	99.64	-5.25
2741-19	lumefantrine	1000	31.25	94.96	99.62	-4.66	94.90	0.00	95.09	-0.19	99.71	-4.82
2741-19	lumefantrine	2000	31.25	95.17	99.62	-4.45	95.92	-1.53	95.09	-0.70	99.77	-5.38
2741-19	lumefantrine	0	15.63	81.89	81.89	0.00	81.89	0.00	81.89	0.00	81.89	0.00
2741-19	lumefantrine	7.8125	15.63	81.48	79.53	1.95	81.89	0.26	84.31	-2.17	78.42	3.72
2741-19	lumefantrine	15.625	15.63	82.88	80.36	2.52	81.89	3.57	86.11	-0.65	79.30	6.16
2741-19	lumefantrine	31.25	15.63	88.75	85.31	3.44	81.89	6.89	89.03	-0.26	85.77	3.01
2741-19	lumefantrine	62.5	15.63	91.62	94.84	-3.23	81.89	12.24	92.06	2.07	94.41	-0.28
2741-19	lumefantrine	125	15.63	95.10	98.44	-3.34	92.86	3.06	93.75	2.17	98.71	-2.79
2741-19	lumefantrine	250	15.63	95.08	98.97	-3.89	93.62	2.30	94.76	1.16	98.84	-2.93
2741-19	lumefantrine	500	15.63	94.89	99.04	-4.14	93.62	0.26	94.87	-0.99	98.84	-4.97
2741-19	lumefantrine	1000	15.63	94.87	99.04	-4.18	94.90	-1.79	95.09	-1.98	99.08	-5.96
2741-19	lumefantrine	2000	15.63	95.10	99.04	-3.94	95.92	-1.02	95.09	-0.19	99.26	-4.36
2741-19	lumefantrine	0	7.81	54.59	54.59	0.00	54.59	0.00	54.59	0.00	54.59	0.00
2741-19	lumefantrine	7.8125	7.81	53.55	49.22	4.33	54.59	-4.59	62.55	-12.55	45.90	4.10
2741-19	lumefantrine	15.625	7.81	54.77	51.26	3.51	54.59	-5.36	68.94	-19.70	48.10	1.13

2741-19	lumefantrine	31.25	7.81	63.66	63.54	0.12	54.59	9.18	78.47	-14.70	64.32	-0.55
2741-19	lumefantrine	62.5	7.81	86.76	87.20	-0.45	69.13	16.58	88.13	-2.42	85.98	-0.27
2741-19	lumefantrine	125	7.81	94.91	96.13	-1.22	92.86	2.55	93.18	2.23	96.76	-1.35
2741-19	lumefantrine	250	7.81	95.22	97.45	-2.23	93.62	1.02	93.97	0.67	97.10	-2.46
2741-19	lumefantrine	500	7.81	95.02	97.61	-2.59	93.62	1.02	94.76	-0.12	97.10	-2.46
2741-19	lumefantrine	1000	7.81	95.03	97.63	-2.60	94.90	-0.51	94.98	-0.59	97.68	-3.30
2741-19	lumefantrine	2000	7.81	95.27	97.63	-2.36	95.92	0.51	95.09	1.34	98.15	-1.72
2741-19	lumefantrine	0	3.91	22.70	22.70	0.00	22.70	0.00	22.70	0.00	22.70	0.00
2741-19	lumefantrine	7.8125	3.91	19.58	11.63	7.95	22.70	-4.85	32.46	-14.61	7.92	9.94
2741-19	lumefantrine	15.625	3.91	21.91	15.19	6.71	22.70	0.00	43.24	-20.54	11.66	11.04
2741-19	lumefantrine	31.25	3.91	36.50	36.57	-0.07	22.70	14.54	62.66	-25.41	39.27	-2.02
2741-19	lumefantrine	62.5	3.91	77.04	77.74	-0.69	69.13	7.91	83.42	-6.38	76.14	0.90
2741-19	lumefantrine	125	3.91	93.82	93.26	0.56	92.86	1.28	92.52	1.62	94.48	-0.35
2741-19	lumefantrine	250	3.91	95.18	95.56	-0.38	93.62	1.79	93.97	1.44	95.07	0.34
2741-19	lumefantrine	500	3.91	95.03	95.84	-0.81	93.62	2.04	94.76	0.90	95.07	0.59
2741-19	lumefantrine	1000	3.91	95.08	95.87	-0.78	94.90	-0.51	94.98	-0.59	96.06	-1.67
2741-19	lumefantrine	2000	3.91	95.32	95.87	-0.55	95.92	-0.87	95.09	-0.04	96.85	-1.79
2741-19	lumefantrine	0	0.00	-5.08	-5.08	0.00	-5.08	0.00	-5.08	0.00	-5.08	0.00
2741-19	lumefantrine	7.8125	0.00	-19.13	-19.13	0.00	-19.13	0.00	-19.13	0.00	-19.13	0.00
2741-19	lumefantrine	15.625	0.00	-14.29	-14.29	0.00	-14.29	0.00	-14.29	0.00	-14.29	0.00
2741-19	lumefantrine	31.25	0.00	21.43	21.43	0.00	21.43	0.00	21.43	0.00	21.43	0.00
2741-19	lumefantrine	62.5	0.00	69.13	69.13	0.00	69.13	0.00	69.13	0.00	69.13	0.00
2741-19	lumefantrine	125	0.00	92.86	92.86	0.00	92.86	0.00	92.86	0.00	92.86	0.00
2741-19	lumefantrine	250	0.00	93.62	93.62	0.00	93.62	0.00	93.62	0.00	93.62	0.00
2741-19	lumefantrine	500	0.00	93.62	93.62	0.00	93.62	0.00	93.62	0.00	93.62	0.00
2741-19	lumefantrine	1000	0.00	94.90	94.90	0.00	94.90	0.00	94.90	0.00	94.90	0.00
2741-19	lumefantrine	2000	0.00	95.92	95.92	0.00	95.92	0.00	95.92	0.00	95.92	0.00

Appendix Table 1: Synergy scores of 2741-19 in combination with lumefantrine in four synergy models. Suffixes that include 'fit' are the experimental or imputed percent inhibition for the drug concentration combination. Suffixes that include 'ref' are the expected inhibition response based on the reference model. The suffix 'synergy' is the synergy score calculated as the difference of 'fit' and 'ref' values.

drug 1	drug2	conc 1	conc 2	ZIP_ fit	ZIP_ ref	ZIP_synergy	HSA_ ref	HSA_synergy	Loewe_ ref	Loewe_synergy	Bliss_ ref	Bliss_synergy
2741-19	piperaquine	250.00	0.00	93.33	93.33	0.00	93.33	0.00	93.33	0.00	93.33	0.00
2741-19	piperaquine	500.00	0.00	94.16	94.16	0.00	94.16	0.00	94.16	0.00	94.16	0.00

2741-19	piperaquine	125.00	0.00	91.73	91.73	0.00	91.73	0.00	91.73	0.00	91.73	0.00
2741-19	piperaquine	62.50	0.00	64.33	64.33	0.00	64.33	0.00	64.33	0.00	64.33	0.00
2741-19	piperaquine	31.25	0.00	21.56	21.56	0.00	21.56	0.00	21.56	0.00	21.56	0.00
2741-19	piperaquine	15.63	0.00	3.46	3.46	0.00	3.46	0.00	3.46	0.00	3.46	0.00
2741-19	piperaquine	0.00	0.00	38.11	38.11	0.00	38.11	0.00	38.11	0.00	38.11	0.00
2741-19	piperaquine	0.98	0.00	-1.69	-1.69	0.00	-1.69	0.00	-1.69	0.00	-1.69	0.00
2741-19	piperaquine	1.95	0.00	-0.78	-0.78	0.00	-0.78	0.00	-0.78	0.00	-0.78	0.00
2741-19	piperaquine	3.91	0.00	-0.09	-0.09	0.00	-0.09	0.00	-0.09	0.00	-0.09	0.00
2741-19	piperaquine	7.81	0.00	-2.15	-2.15	0.00	-2.15	0.00	-2.15	0.00	-2.15	0.00
2741-19	piperaquine	250.00	0.39	96.67	93.53	3.14	93.33	2.16	93.65	1.84	92.53	2.96
2741-19	piperaquine	500.00	0.39	97.12	94.33	2.79	94.16	-0.98	94.35	-1.16	93.43	-0.25
2741-19	piperaquine	125.00	0.39	93.89	89.59	4.30	91.73	4.50	89.51	6.72	90.93	5.29
2741-19	piperaquine	62.50	0.39	77.39	68.71	8.68	64.33	17.88	71.85	10.37	60.03	22.18
2741-19	piperaquine	31.25	0.39	39.66	23.01	16.65	22.03	14.69	24.39	12.33	12.04	24.68
2741-19	piperaquine	15.63	0.39	8.86	10.03	-1.17	3.46	5.72	9.60	-0.42	-8.76	17.94
2741-19	piperaquine	0.00	0.39	-11.97	-11.97	0.00	-11.97	0.00	-11.97	0.00	-11.97	0.00
2741-19	piperaquine	0.98	0.39	-6.70	6.82	-13.52	-1.69	-1.18	5.86	-8.73	-14.46	11.59
2741-19	piperaquine	1.95	0.39	-5.93	6.84	-12.77	-0.78	0.51	5.86	-6.13	-13.43	13.17
2741-19	piperaquine	3.91	0.39	-4.58	6.93	-11.51	-0.09	1.90	5.86	-4.06	-12.66	14.46
2741-19	piperaquine	7.81	0.39	-2.46	7.41	-9.87	-2.15	8.92	6.35	0.41	-14.98	21.74
2741-19	piperaquine	250.00	0.78	98.69	93.54	5.15	93.33	5.85	97.56	1.62	92.86	6.32
2741-19	piperaquine	500.00	0.78	97.58	94.34	3.24	94.16	2.71	94.35	2.53	93.72	3.16
2741-19	piperaquine	125.00	0.78	96.64	89.60	7.04	91.73	7.70	96.65	2.77	91.33	8.09
2741-19	piperaquine	62.50	0.78	82.02	68.75	13.27	64.33	17.14	74.49	6.99	61.79	19.69
2741-19	piperaquine	31.25	0.78	40.81	23.10	17.71	22.55	20.07	27.14	15.48	15.90	26.72
2741-19	piperaquine	15.63	0.78	5.58	10.13	-4.55	3.70	2.28	10.98	-5.00	-3.99	9.97
2741-19	piperaquine	0.00	0.78	-7.05	-7.05	0.00	-7.05	0.00	-7.05	0.00	-7.05	0.00
2741-19	piperaquine	0.98	0.78	-4.35	6.94	-11.28	-1.69	2.66	5.86	-4.90	-9.43	10.40
2741-19	piperaquine	1.95	0.78	-3.82	6.95	-10.78	-0.78	0.12	5.86	-6.52	-8.45	7.79
2741-19	piperaquine	3.91	0.78	-3.33	7.04	-10.37	-0.09	2.58	5.86	-3.37	-7.71	10.20
2741-19	piperaquine	7.81	0.78	-3.28	7.52	-10.80	-2.15	-1.61	6.75	-10.51	-9.93	6.17
2741-19	piperaquine	250.00	1.56	99.14	93.58	5.56	93.33	4.86	95.50	2.70	92.94	5.26
2741-19	piperaquine	500.00	1.56	98.16	94.37	3.79	94.16	4.52	96.58	2.10	93.79	4.90
2741-19	piperaquine	125.00	1.56	97.14	89.69	7.45	91.73	7.21	94.49	4.44	91.43	7.50

2741-19	piperaquine	62.50	1.56	83.67	69.01	14.66	64.33	22.55	78.60	8.28	62.22	24.66
2741-19	piperaquine	31.25	1.56	45.31	23.65	21.66	22.81	21.04	34.49	9.36	16.87	26.98
2741-19	piperaquine	15.63	1.56	8.57	10.80	-2.23	3.83	5.59	14.43	-5.00	-2.79	12.21
2741-19	piperaquine	0.00	1.56	-5.82	-5.82	0.00	-5.82	0.00	-5.82	0.00	-5.82	0.00
2741-19	piperaquine	0.98	1.56	-3.55	7.63	-11.17	-1.69	6.20	5.86	-1.36	-8.18	12.68
2741-19	piperaquine	1.95	1.56	-2.82	7.64	-10.47	-0.78	-0.52	5.86	-7.16	-7.20	5.91
2741-19	piperaquine	3.91	1.56	-2.48	7.73	-10.21	-0.09	-3.27	6.36	-9.72	-6.47	3.11
2741-19	piperaquine	7.81	1.56	-2.17	8.21	-10.38	-2.15	7.74	8.23	-2.64	-8.66	14.25
2741-19	piperaquine	250.00	3.13	98.38	93.89	4.50	93.33	5.36	96.29	2.40	93.37	5.32
2741-19	piperaquine	500.00	3.13	97.46	94.64	2.83	94.16	2.17	94.44	1.89	94.17	2.17
2741-19	piperaquine	125.00	3.13	96.88	90.23	6.64	91.73	6.47	93.52	4.67	91.95	6.25
2741-19	piperaquine	62.50	3.13	84.91	70.66	14.24	64.33	20.83	83.42	1.75	64.51	20.66
2741-19	piperaquine	31.25	3.13	47.85	27.39	20.47	24.14	19.47	52.89	-9.29	21.89	21.71
2741-19	piperaquine	15.63	3.13	14.40	15.25	-0.85	4.50	10.83	27.28	-11.95	3.42	11.91
2741-19	piperaquine	0.00	3.13	0.57	0.57	0.00	0.57	0.00	0.57	0.00	0.57	0.00
2741-19	piperaquine	0.98	3.13	1.48	12.27	-10.78	0.57	-2.07	8.74	-10.24	-1.64	0.15
2741-19	piperaquine	1.95	3.13	3.08	12.28	-9.20	0.57	9.39	9.73	0.24	-0.73	10.69
2741-19	piperaquine	3.91	3.13	2.19	12.36	-10.17	0.57	-5.51	11.89	-16.83	-0.04	-4.90
2741-19	piperaquine	7.81	3.13	2.05	12.81	-10.76	0.57	-6.59	16.21	-22.23	-2.10	-3.92
2741-19	piperaquine	250.00	6.25	97.35	95.75	1.60	93.33	4.13	94.25	3.21	95.78	1.68
2741-19	piperaquine	500.00	6.25	97.13	96.27	0.86	94.16	2.52	94.54	2.14	96.36	0.32
2741-19	piperaquine	125.00	6.25	94.51	93.24	1.28	91.73	1.04	93.55	-0.78	95.08	-2.31
2741-19	piperaquine	62.50	6.25	79.81	79.79	0.02	64.48	5.25	88.63	-18.90	77.91	-8.19
2741-19	piperaquine	31.25	6.25	55.11	49.39	5.72	41.79	11.52	78.35	-25.04	51.53	1.78
2741-19	piperaquine	15.63	6.25	45.82	41.02	4.80	38.09	12.42	61.64	-11.12	39.80	10.71
2741-19	piperaquine	0.00	6.25	38.09	38.09	0.00	38.09	0.00	38.09	0.00	38.09	0.00
2741-19	piperaquine	0.98	6.25	33.74	38.96	-5.22	38.09	-7.56	37.42	-6.89	36.53	-6.01
2741-19	piperaquine	1.95	6.25	36.23	38.97	-2.74	38.09	-5.96	39.27	-7.14	37.11	-4.98
2741-19	piperaquine	3.91	6.25	33.57	39.03	-5.45	38.09	-6.42	42.59	-10.92	37.53	-5.86
2741-19	piperaquine	7.81	6.25	33.92	39.34	-5.42	38.09	-7.33	49.23	-18.47	36.25	-5.49
2741-19	piperaquine	250.00	12.50	97.39	98.97	-1.58	93.33	6.67	98.67	1.33	98.77	1.23
2741-19	piperaquine	500.00	12.50	96.82	99.10	-2.28	94.16	-0.72	94.74	-1.30	98.92	-5.48
2741-19	piperaquine	125.00	12.50	96.52	98.32	-1.80	91.73	2.73	94.05	0.41	98.54	-4.08
2741-19	piperaquine	62.50	12.50	90.41	95.06	-4.65	83.10	7.38	93.26	-2.78	93.54	-3.06

2741-19	piperaquine	31.25	12.50	83.30	87.56	-4.26	81.63	4.20	91.49	-5.66	85.56	0.26
2741-19	piperaquine	15.63	12.50	83.05	85.45	-2.39	81.63	0.77	89.63	-7.23	82.13	0.27
2741-19	piperaquine	0.00	12.50	81.63	81.63	0.00	81.63	0.00	81.63	0.00	81.63	0.00
2741-19	piperaquine	0.98	12.50	81.44	84.91	-3.48	81.63	-1.51	84.65	-4.53	81.20	-1.08
2741-19	piperaquine	1.95	12.50	81.24	84.92	-3.68	81.63	0.32	85.04	-3.09	81.37	0.58
2741-19	piperaquine	3.91	12.50	81.04	84.93	-3.89	81.63	-3.56	86.01	-7.95	81.49	-3.43
2741-19	piperaquine	7.81	12.50	80.84	85.01	-4.18	81.63	-3.79	87.57	-9.74	81.11	-3.28
2741-19	piperaquine	250.00	25.00	98.59	99.81	-1.21	98.01	0.75	97.78	0.99	99.87	-1.10
2741-19	piperaquine	500.00	25.00	98.25	99.83	-1.58	98.01	1.12	97.87	1.26	99.88	-0.75
2741-19	piperaquine	125.00	25.00	98.18	99.69	-1.51	98.62	0.26	97.87	1.00	99.84	-0.97
2741-19	piperaquine	62.50	25.00	96.39	99.07	-2.68	98.01	0.50	97.76	0.75	99.33	-0.82
2741-19	piperaquine	31.25	25.00	95.44	97.68	-2.24	98.01	-0.13	97.37	0.52	98.43	-0.54
2741-19	piperaquine	15.63	25.00	97.14	97.26	-0.12	98.01	-0.36	97.17	0.48	98.07	-0.42
2741-19	piperaquine	0.00	25.00	98.01	98.01	0.00	98.01	0.00	98.01	0.00	98.01	0.00
2741-19	piperaquine	0.98	25.00	97.59	97.16	0.42	98.01	0.39	97.12	1.28	97.96	0.44
2741-19	piperaquine	1.95	25.00	97.87	97.16	0.71	98.01	0.61	97.24	1.39	97.98	0.65
2741-19	piperaquine	3.91	25.00	97.85	97.17	0.68	98.01	0.16	97.19	0.98	97.99	0.18
2741-19	piperaquine	7.81	25.00	97.54	97.18	0.36	98.01	-0.07	97.15	0.79	97.95	-0.01
2741-19	piperaquine	250.00	50.00	98.82	99.90	-1.08	99.21	0.08	98.47	0.82	99.95	-0.67
2741-19	piperaquine	500.00	50.00	98.70	99.91	-1.21	99.08	-0.30	98.27	0.51	99.95	-1.17
2741-19	piperaquine	125.00	50.00	98.52	99.85	-1.33	99.51	-0.12	98.37	1.03	99.94	-0.55
2741-19	piperaquine	62.50	50.00	97.63	99.53	-1.90	99.08	-0.07	98.27	0.74	99.67	-0.67
2741-19	piperaquine	31.25	50.00	98.03	98.80	-0.77	99.08	-0.29	98.36	0.43	99.43	-0.65
2741-19	piperaquine	15.63	50.00	98.97	98.59	0.39	99.08	-0.80	98.07	0.22	99.06	-0.78
2741-19	piperaquine	0.00	50.00	99.08	99.08	0.00	99.08	0.00	99.08	0.00	99.08	0.00
2741-19	piperaquine	0.98	50.00	99.25	98.54	0.71	99.08	0.69	98.45	1.32	99.05	0.72
2741-19	piperaquine	1.95	50.00	99.91	98.54	1.37	99.08	0.92	98.46	1.54	99.06	0.94
2741-19	piperaquine	3.91	50.00	99.56	98.54	1.02	99.08	1.15	98.47	1.76	99.07	1.16
2741-19	piperaquine	7.81	50.00	99.26	98.55	0.71	99.08	1.15	98.49	1.74	99.05	1.18
2741-19	piperaquine	250.00	100.00	98.79	99.91	-1.12	98.77	-1.11	98.67	-1.01	99.91	-2.26
2741-19	piperaquine	500.00	100.00	98.96	99.92	-0.96	98.77	1.15	98.67	1.25	99.93	-0.01
2741-19	piperaquine	125.00	100.00	98.53	99.87	-1.33	99.18	0.16	98.67	0.68	99.90	-0.56
2741-19	piperaquine	62.50	100.00	98.37	99.58	-1.22	98.77	0.12	98.67	0.22	99.54	-0.66
2741-19	piperaquine	31.25	100.00	99.49	98.92	0.57	98.77	-0.34	98.67	-0.24	99.01	-0.58

2741-19	piperaquine	15.63	100.00	99.24	98.74	0.49	98.77	1.00	98.66	1.11	98.79	0.98
2741-19	piperaquine	0.00	100.00	98.77	98.77	0.00	98.77	0.00	98.77	0.00	98.77	0.00
2741-19	piperaquine	0.98	100.00	99.04	98.70	0.33	98.77	-1.05	98.67	-0.95	98.73	-1.01
2741-19	piperaquine	1.95	100.00	99.80	98.70	1.10	98.77	1.69	98.64	1.82	98.74	1.72
2741-19	piperaquine	3.91	100.00	99.39	98.70	0.69	98.77	1.00	98.66	1.11	98.75	1.02
2741-19	piperaquine	7.81	100.00	99.12	98.71	0.41	98.77	0.09	98.67	0.19	98.72	0.14
2741-19	piperaquine	250.00	200.00	98.56	99.91	-1.35	98.55	-0.61	98.67	-0.73	99.90	-1.96
2741-19	piperaquine	500.00	200.00	98.99	99.92	-0.93	98.55	0.30	98.67	0.18	99.91	-1.06
2741-19	piperaquine	125.00	200.00	98.37	99.87	-1.50	99.00	-0.07	98.67	0.26	99.88	-0.96
2741-19	piperaquine	62.50	200.00	98.93	99.59	-0.66	98.55	-0.60	98.67	-0.72	99.48	-1.54
2741-19	piperaquine	31.25	200.00	100.48	98.94	1.53	98.55	0.77	98.67	0.65	98.86	0.46
2741-19	piperaquine	15.63	200.00	99.15	98.76	0.39	98.55	0.22	98.67	0.10	98.59	0.18
2741-19	piperaquine	0.00	200.00	98.55	98.55	0.00	98.55	0.00	98.55	0.00	98.55	0.00
2741-19	piperaquine	0.98	200.00	98.87	98.72	0.15	98.55	-0.07	98.67	-0.19	98.52	-0.04
2741-19	piperaquine	1.95	200.00	99.65	98.72	0.92	98.55	0.56	98.67	0.44	98.53	0.58
2741-19	piperaquine	3.91	200.00	99.23	98.73	0.50	98.55	0.81	98.67	0.69	98.54	0.82
2741-19	piperaquine	7.81	200.00	98.96	98.73	0.23	98.55	-0.47	98.67	-0.59	98.51	-0.43

Appendix Table 2: Synergy scores of 2741-19 in combination with piperaquine in four synergy models.
Suffixes that include ‘fit’ are the experimental or imputed percent inhibition for the drug concentration combination. Suffixes that include ‘ref’ are the expected inhibition response based on the reference model. The suffix ‘synergy’ is the synergy score calculated as the difference of ‘fit’ and ‘ref’ values.